J. Fluid Mech. (1990), *vol.* 212, *pp.* 497–532
Printed in Great Britain

Rapid distortion theory and the 'problems' of turbulence

By J. C. R. HUNT AND D. J. CARRUTHERS
Department of Applied Mathematics and Theoretical Physics, University of Cambridge, Silver Street, Cambridge CB3 9EW, UK

(Received 3 August 1989)

The 'problems' associated with analysing different kinds of turbulent flow and different methods of solution are classified and discussed with reference to how the turbulent structure in a flow domain depends on the scale and geometry of the domain's boundary, and on the information provided in the boundary conditions. Rapid distortion theory (RDT) is a method, based on linear analysis, for calculating 'rapidly changing turbulent' (RCT) flows under the action of different kinds of distortion, such as large-scale velocity gradients, the effects of bounding surfaces, body forces, etc. Recent developments of the theory are reviewed, including the criteria for its validity, and new solutions allowing for the effects of inhomogeneities and boundaries.

We then consider the contribution of RDT to understanding the fundamental problems of 'slowly changing turbulent' (SCT) flows, such as why are similar and persistent features of the local eddy structure found in different kinds of shear flow, and what are the general features of turbulent flows near boundaries. These features, which can be defined in terms of certain statistical quantities and flow patterns in individual flow realizations, are found to correspond to the form of particular solutions of RDT which change slowly over the time of the distortion. The most general features are insensitive to the energy spectrum and to the initial anisotropy of the turbulence. A new RDT analysis of the energy spectra $E(k)$ indicates why, in shear flows at moderate Reynolds number, the turbulence tends to have similar forms of spectra for eddies on a local scale, despite the Reynolds number not being large enough for the existence of a nonlinear cascade and there being no universal forms of spectra for unsheared turbulence; for this situation, the action of shear $\mathrm{d}U_1/\mathrm{d}x_2$ changes the form of the spectrum, so that, as $\beta = (t\,\mathrm{d}U_1/\mathrm{d}x_2)$ increases, over an increasing part of the spectrum defined in terms of the integral scale L by $\beta^{-1} \gg kL, E(k) \propto k^{-2}$, whatever the form of initial spectrum of $E_0(k)$ (provided $E(k) = o(k^{-2})$ for $kL \gg 1$).

1. Introduction

Although George Batchelor said that he moved on from his studies of turbulence to other fields of fluid mechanics in the early 1960's, he has continued to maintain a close interest in turbulence research, and his shrewd understanding has always been available to those who have consulted him. He summarized his view on 'the problems of turbulence' in a sentence or two in his recent opening introduction to the first European Turbulence Conference at Lyon in 1986 (Comte-Bellot & Mathieu 1987), where he predicted that there could be no global theory of turbulence (other than that turbulent flows are governed by the Navier–Stokes equations) because all

turbulent flows to a greater or lesser extent are determined by their initial and boundary conditions. This negative statement does not exclude the fact that there are important features that are common to many different types of turbulent flows at high Reynolds number. This was really a reaffirmation of the ideas so clearly explained in Chapter 6 'Universal Equilibrium Theory' of Batchelor's *Homogeneous Turbulence* (1953), and in the discussion of the final stage of decay.

That book also describes the 'Rapid Distortion Theory' (or RDT) developed by Batchelor & Proudman (1954) for calculating how turbulence is distorted when it passes rapidly through a region of large-scale straining motions. The technique of linearized analysis of the vorticity equation, formulating the random Fourier transforms of the velocity field and thence the spectra, was applied there to study the effect of irrotational strain on initially isotropic homogeneous turbulence, such as occurs in wind-tunnel contractions. Although there was no hint that the linear methods of RDT might provide some insight into turbulence structure, the paper by Pearson (1959), a student in Batchelor's group, showed how RDT could be applied to the distortion of turbulence in shear flows and how it might provide a technique for studying the structure of turbulence, especially shear flow. Since then Craya (1958), Deissler (1968), Townsend (1976), Jeandel, Brison & Mathieu (1978) and most recently Lee, Kim & Moin (1988), have demonstrated by comparison with experiments that the linear theory of rapidly distorted flows can be applied to analysing the structure of slowly changing turbulent shear flows! (See also the recent review by Savill (1987), which focuses on the connection between RDT and other models of turbulence.)

The first purpose of this paper is to review how RDT has been extended to analyse inhomogeneous turbulent flows, including some effects of boundaries, how some of its mathematical restrictions have been defined and overcome, and how, following Lee *et al.* (1988) RDT not only provides a technique for calculating the second-order moments or spectra of the turbulent velocity field, but also the random realizations of the distorted velocity fields from which characteristic eddy structures can be deduced. The second purpose is to use these developments in RDT and related studies of nonlinear aspects of turbulence to give some new results and insights into the spectra of turbulent shear flows and the corresponding physical structure of eddies governed by the local mean shear.

Because turbulent flows become uncorrelated over time and space, and because they are intrinsically nonlinear, as is evident from their intermittent structure, one might expect that the structure of turbulence depends only weakly upon the boundary and initial conditions. Therefore if asked whether turbulent flows could be analysed by the linear theory of rapidly distorted flows, one would think 'no'. Most solutions in linear theory are generally directly related to the initial conditions and boundary conditions. But the answer may be a qualified 'yes', because some linear solutions may have certain properties that are strictly independent of these conditions ('eigensolutions') or are weakly dependent after statistical averaging ('statistical eigensolutions').

The finite spatial correlation of turbulence might also suggest that turbulence is dominated by the local mean flow variations (and the presence of nearby surfaces) rather than the structure of the whole mean flow profile. This is the approach used in the analysis of turbulent flows by models of the statistical moments (whose methodology was set out by Lumley 1978). This local approach logically implies that there is a common structure found in all turbulent shear flows. By showing that certain ratios of Reynolds stress change slowly with time (or distance) Townsend

(1976) and Jeandel *et al.* (1978) argued that these ratios demonstrated the common structure. There is also evidence that the coherent structures or characteristic eddies obtained by sampling the flow also have certain common features in different kinds of fully developed shear flow (Hussain 1986). (These remarks are not related to Kolmogorov's model of a universal structure for the small scales of turbulence when the Reynolds number is large enough that the largest straining rates are induced by the smallest scales of turbulence.)

But can a model for the distortion of turbulence by a uniform shear be applicable to naturally occurring turbulent shear flows (such as boundary layers, jets and wakes) which are significantly inhomogeneous on a scale comparable with that of the scale of the eddies? The answer is also a qualified 'yes'. Townsend (1976) and others (e.g. Maxey 1982; Savill 1987; Lee *et al.* 1988; Landahl 1990) have shown that many features of turbulent wakes, pipe flows and boundary layers can be described by RDT for homogeneous turbulence in a uniform shear. The general validity of this approximation can now be examined using the recent extension of RDT to inhomogeneous flows.

An alternative theoretical approach to studying the essential large-scale structure of turbulence is to use the techniques of linear stability theory (e.g. Liu 1989) to calculate the eigenmodes of the mean velocity field, either the neutral (Lessen 1979) or the fastest-growing eigenmodes (Ho & Huerre 1984; Gaster, Kit & Wygnanski 1985). These discrete eigenmodes are large scale and span the whole flow field and are therefore special to that particular turbulent flow. In the early stages of shear flows when there have been only a few nonlinear interactions between the structures (e.g. Ho & Huerre 1984) it is found that their amplitude and phase distribution correspond approximately to the large-scale features of the nonlinear 'coherent structures'; but the smaller-scale motions within these structures and smaller-scale substructures are not well modelled by these eigenmodes of the whole flow (Hussain 1986). These large-scale motions, which are characteristic of the whole flow, do not in most shear flows account for a significant proportion of the energy and momentum of the turbulent motions by comparison with the generic turbulent motions on the local scale of the mean shear (e.g. defined by $u_0/\mathrm{d}U_1/\mathrm{d}x_2$, where u_1 is related to the local r.m.s. velocity and $U_1(x_2)$ is the mean velocity profile). But the large-scale motions can account for a high proportion of the energy and momentum in the presence of external forcing of the flow (e.g. by sound acting on a jet) and they usually play a significant role in transport of scalars, or particles, and in the generation of sound (Hussain 1983).

In this paper we focus on the local-scale motions (but still much larger than any smallest-scale isotropic motions) that are determined by the local shear and by the presence of nearby boundaries. Our aim is to explore further the concepts of a generic or common structure in the energy-containing range of shear-flow turbulence. It is suggested that this structure is equivalent to a 'statistical eigensolution' to the linear RDT analysis. The characteristic structures formed at these local scales are found to be the dominant form of coherent structures in mature shear flows (e.g. in wakes hundreds of diameters downwind of the obstacle; Mumford 1982; Férre & Giralt 1989; Hayakawa & Hussain 1989).

In §2 we classify and discuss the different kinds of turbulence 'problems' to indicate where different kinds of turbulence theory might be applicable and what we mean by rapid and slowly changing turbulent flows. In §3 we review developments in RDT, and in §4 we present our new results and a review of shear flows.

2. Turbulent flow problems: boundary and initial conditions and methods of solution

2.1. *Boundary and initial conditions*

A turbulent flow occurs in a domain $\mathscr{D}$ if the Reynolds number Re, based on the variation of the local mean velocity U_0 and the lengthscale $L_{\mathscr{D}}$ of $\mathscr{D}$, is great enough that either laminar flows are unstable (at the level of local disturbances advected into $\mathscr{D}$ or generated by body forces), or if turbulent flows advected into this domain do not decay.

As in other fluid-mechanical problems, the solution of problems of turbulent flow require specification of boundary or initial conditions for the domain and time period in question. But unlike deterministic problems in fluid mechanics, in many problems in turbulence these boundary conditions on the turbulence are not known sufficiently well to define the full turbulent velocity field $T\{\boldsymbol{u}\}$ in $\mathscr{D}$ (for example in weather forecasting). In some problems these turbulent boundary conditions do not need to be known (e.g. fully developed turbulent flow along a pipe far from the entry is independent of the incoming turbulence), and in others these conditions need only be known to a limited extent (e.g. up to a certain order of moments), if only limited information is required about the mean and turbulent velocity field. However, it is not clear in general how much information about the boundary conditions is needed to derive the required level of information about $T\{\boldsymbol{u}\}$. The essential feature of the turbulent velocity field is that any single realization is very sensitive to small changes in the initial or boundary conditions, and effectively cannot be computed if the conditions are specified too long before or too far away. (This is the problem of predictability discussed by Leith 1978 and Tennekes 1988.)

In most practical problems where a turbulent velocity field has to be calculated or defined in terms of experimental measurements, the usual objective is to estimate or measure the ensemble or time mean of the moments (up to order k) denoted by $\overline{M_k}$, in terms of mean moments (up to order l), of the velocity field at the initial moment $\overline{M_l}^{(0)}(\boldsymbol{u}^{(0)};\ldots)$ (denoted by $\overline{M_l}^{(0)}$), and, over some part of the bounding surface $\overline{M_m}(\boldsymbol{u}^{(\mathscr{B})};\ldots)$ (denoted by $\overline{M_m}^{(\mathscr{B})}$. In some cases (e.g. in closed domains, such as electromagnetically driven turbulent flows; Davidson, Hunt & Moros 1988) $\overline{M_k}$ is also determined by the nth moments of applied body forces over the domain, $\overline{M_n}^{(f)}$.

How much information about $\overline{M_l}^{(0)}$ and $\overline{M_m}^{(\mathscr{B})}$ is needed for a required level of accuracy of computation of the kth-order moments in a particular flow? Depending on the nature of the turbulent flow and depending on the elapsed time of the flow and lengthscale of the flow domain, it may be necessary to specify moments of higher order than k (where $l, m > k$) or it may be sufficient to specify moments of lower order (where $l, m < k$) of the velocity field defined initially and on $\mathscr{B}$. These are not academic questions.

Suppose the second-order moments $\overline{M_2}$ of the wind speed are required at a point $\boldsymbol{x}$ in a complex flow (e.g. on a hill top or in some fluid-flow machinery) where there is information about the turbulence at $\boldsymbol{x}_s$ upstream of that point, and it is known that this turbulence is correlated with the turbulence at $\boldsymbol{x}$. What is the connection between $\overline{M_2}$ at $\boldsymbol{x}$ and the moments $\overline{M_m}^{(s)}$ at the upstream points ($\boldsymbol{x}_s$)? Is it necessary to measure beyond $m = 2$, and how close should $\boldsymbol{x}_s$ be to $\boldsymbol{x}$ for a given level of accuracy of predicting $\overline{M_2}$ for a given value of m?

This is a problem of 'rapidly changing turbulent' flow (RCT), where one is just

asking how the turbulence changes. One is not asking fundamental questions about the nature and the causes of the structure of the turbulent flow at $\boldsymbol{x}$.

But the usual 'problems' concern flows with slowly changing turbulence (SCT) which occur over long periods in large flow domains. Typically such a problem can be stated as: given the first moments (i.e. the mean velocity field $\overline{M_1}^{(0)}$ or $\overline{M_1}^{(s)}$), and the boundary conditions, determine all the moments and probability distribution of the velocity field $\overline{M_k}$ for $k = 1, 2, \ldots$ (including, for example, the form and magnitude of the small-scale universal spectra of turbulence). This is generally regarded as a 'fundamental' question, because it asks what is the structure (as defined by second- and higher-order moments) that is independent of the initial state of the turbulence and independent of turbulence that is transported into the domain across boundaries.

A simple classification of turbulent flows in terms of their initial and boundary conditions shows how some are rapidly changing and some are slowly changing flows. We also see how different regions and features of the *same* flow can be understood and analysed in terms of these different simplifying limits.

Class I. *Closed domains and deterministic boundary conditions*

In these turbulent flows the boundary surface $\mathscr{B}$ of the domain $\mathscr{D}$ of the flow consists of rigid stationary or moving surfaces moving with a velocity $\boldsymbol{U}^{(b)}(\boldsymbol{x}, t)$, with a typical scale of $U_{\mathscr{B}}$. Turbulent motion is either caused by non-uniform motion of the boundaries (as in a cylinder with a moving piston or oscillating grid in a box, or a mixer with an impeller, figure 1), or by the action of body forces $\boldsymbol{f}(\boldsymbol{x}_1, t)$ (as with thermal convection on a surface or electromagnetic forcing in furnaces). The body forces may be unsteady. After a long time, whether or not there is any initial motion, (so that $\boldsymbol{u}^{(0)}$ is irrelevant), the turbulence (and all its statistics $\overline{M_k}(\boldsymbol{u}; \ldots)$) is solely determined by instabilities of the mean motions and the action of body forces. But the only non-zero boundary conditions that determine the mean motion and the turbulence are the distributions of the mean velocity on $\mathscr{B}$ and/or force $\boldsymbol{f}$ throughout $\mathscr{D}$.

Class II. *Open domains and statistical boundary conditions*

In this class of turbulent flows, some of the bounding surface of the flow domain $\mathscr{D}$ lies within the fluid and, in general, there is some motion across $\mathscr{B}$, i.e. $\boldsymbol{u}^{(\mathscr{B})} \cdot \boldsymbol{n}^{(\mathscr{B})} \neq 0$, where $\boldsymbol{n}^{(\mathscr{B})}$ is the outward normal to $\mathscr{B}$. There are two main subclasses depending on the nature of the flow in the region $\mathscr{E}$ outside $\mathscr{D}$.

Class II.1 *No turbulence in* $\mathscr{E}$. In this class the flow entering $\mathscr{D}$, with characteristic mean velocity U_0, is not turbulent, but turbulence is generated within $\mathscr{D}$ by instabilities if Re is large enough (figure 2*a*). This might be a steady uniform flow approaching an aerofoil, or entering a pipe. This class is not quite similar to I because in some flows the moments of turbulence are not only determined by the mean motion entering $\mathscr{D}$, and the mean velocity of the boundaries, but also by conditions on the turbulence where the flow leaves $\mathscr{B}$, for example where turbulent flows separate from sharp edges.

Class II.2 *Turbulence in* $\mathscr{E}$. This class must be divided into two subclasses.

Class II.2.1 *Significant mean flow from* $\mathscr{E}$ *through* $\mathscr{D}$. In this case, turbulence generated in $\mathscr{E}$ (with typical magnitude u_0) is transported into the region $\mathscr{D}$ by the mean velocity field $\boldsymbol{U}(\boldsymbol{x}, t)$ with typical magnitude U_0. This implies that there is a component of the mean flow normal to $\mathscr{B}$ which is significantly greater than the turbulence, i.e. $\boldsymbol{U} \cdot \boldsymbol{n}^{(\mathscr{B})} \neq 0$ and $U_0 \cos \alpha^{(\mathscr{B})} \geqslant u_0$, where $\alpha^{(\mathscr{B})}$ is the angle between $\boldsymbol{U}$ and $\boldsymbol{n}^{(\mathscr{B})}$ (see figure 2*b*).

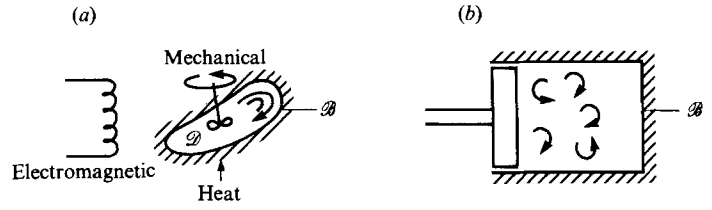

FIGURE 1. Examples of closed domain and deterministic boundary conditions. (*a*) Forced mixing with an impeller or body forces (electromagnetic or buoyancy); (*b*) a cylinder with a moving piston.

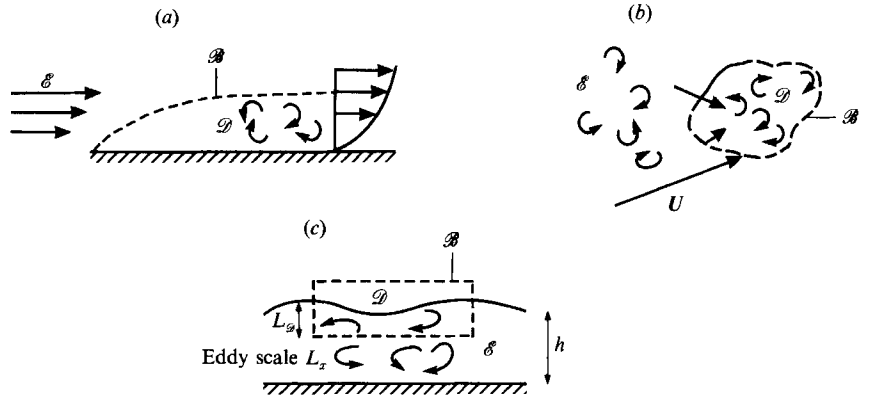

FIGURE 2. Open domains and statistical boundary conditions. (*a*) Flow entering $\mathscr{D}$ is not turbulent; turbulence generated within $\mathscr{D}$. (*b*) Turbulence in $\mathscr{E}$ advected into $\mathscr{D}$ by mean flow across $\mathscr{B}$. (*c*) Random motion across bounding surface $\mathscr{B}$ advects turbulence into $\mathscr{D}$.

The integral lengthscale of the turbulence transported into $\mathscr{D}$ is L_x, and thence the integral ('Lagrangian' or 'turn-over') timescale T_L can be estimated. For most well-developed high-Reynolds-number turbulent flows $T_L \sim L_x/u_0$ (e.g. Tennekes & Lumley 1971). If $L_{\mathscr{D}}$ is the distance along the streamlines of the mean flow through $\mathscr{D}$, the travel time of a turbulent eddy is $T_{\mathscr{D}} \sim L_{\mathscr{D}}/U_0$. The ratio $T_{\mathscr{D}}/T_L$ can be used to divide these kinds of turbulent flows, through 'open' control surfaces, into flows with 'rapidly changing turbulence' when $T_{\mathscr{D}}/T_L \sim L_{\mathscr{D}} u_0/(L_x U_0) \ll 1$, and 'slowly changing turbulence' when $T_{\mathscr{D}}/T_L \sim L_{\mathscr{D}} u_0/(L_x U_0) \gtrsim 1$.

In most turbulent flows L_x and U_0 decrease rapidly near rigid surfaces so the ratio $T_{\mathscr{D}}/T_L$ may be small in the interior of the flow and large near rigid surfaces. Since this ratio is proportional to $L_{\mathscr{D}}$, the choice of the size of the flow domain also determines the kind of turbulent problem, and whether it is an RCT or an SCT problem.

There are many important examples of turbulent flows which have been studied intensively both theoretically and experimentally in the framework of rapidly changing turbulent flows (RCT), i.e. studying the changes of the turbulence in terms of the distortion they undergo in $\mathscr{D}$ and the nature of the turbulence being advected into $\mathscr{D}$. These include the distortion of turbulence in a wind-tunnel contraction (Batchelor & Proudman 1954; Tucker & Reynolds 1968; Goldstein & Durbin 1980), turbulent flows impinging onto aerofoils, flat plates (Goldstein & Atassi 1976; Thomas & Hancock 1977; Hunt & Graham 1978), turbulence passing through wire gauzes, and in compression, shocks, flames and other entropic discontinuities (Taylor & Batchelor 1949; Batchelor 1955; Goldstein 1978; Dussage & Gaviglio 1981), turbulent boundary-layer flows in large pressure gradients or over surface

perturbations, such as hills (Britter, Hunt & Richards 1981; Mason & King 1985; Zeman & Jensen 1987; Hunt, Newley & Weng 1989). For the latter case of distorted boundary layers over rigid surfaces (or 'walls') several studies have now shown how the changes in the structure of the turbulence are quite different near the wall where $T_{\mathscr{D}}/T_{\mathrm{L}} \gtrsim 1$, and in the interior of the flow where $T_{\mathscr{D}}/T_{\mathrm{L}} \lesssim 1$.

Class II.2.2 *No significant mean flow through* $\mathscr{D}$. In these flows the turbulence in $\mathscr{E}$ interacts with or drives the turbulent flow in $\mathscr{D}$ largely by means of random motions across the bounding surface $\mathscr{B}$ (figure 2*c*). The turbulence in $\mathscr{D}$ differs from that in $\mathscr{E}$ because of some distorting effect. It is assumed that any mean flow across $\mathscr{B}$ is weak relative to the turbulence, i.e. $U_0 \cos\alpha \lesssim u_0$. Where the mean shear in $\mathscr{D}$ is small, then it may be useful to define $\mathscr{D}$ in a coordinate system moving with the local mean flow.

These regions of distorted turbulent flows occur at the outer edge of boundary layers (Phillips 1955), in turbulent flows of liquids near a free surface (Hunt 1984) or in stratified flows near density interfaces (Carruthers & Hunt 1986), or in laboratory grid turbulence near a moving wall (Uzkan & Reynolds 1967; Thomas & Hancock 1977), or when external turbulence interacts with the boundary layer on a surface. In most of these cases the changes to the turbulence generated within $\mathscr{D}$ can be comparable with the turbulence in $\mathscr{E}$.

When a discontinuity is imposed on a turbulent flow, such as a rigid surface or a density discontinuity, and it is imposed instantaneously, its effects typically extends a distance of order of the integral scale of the turbulence L_x. Therefore these regions $\mathscr{D}$ where the changes occur extend a distance of order of L_x from the discontinuities. In some cases where this distance is small compared with the overall scale of the external flow h (as in the convective boundary layer where the thickness h is about $5L_x$), the structure of the turbulence in $\mathscr{D}$ can approximately be considered independently of the turbulence in the whole flow. In other cases this approximation may not be appropriate (as for example in the flow at the top of an unstratified turbulent boundary layer).

For flow regions of this form it follows that the timescale $T_{\mathscr{D}}$ for an eddy to traverse the flow region is typically of order of L_x/u_0, which is of the same order as the natural timescale of the turbulence T_{L}. Therefore, as an eddy impacts on the discontinuity, it is virtually a 'rapid' effect. The advantage of considering small subdomains of this sort in flows is that it may be possible to consider the external turbulence in $\mathscr{E}$ without considering $\mathscr{D}$, and then to consider how the local structure of turbulence in $\mathscr{D}$ is determined by the external turbulence for given kinds of boundary conditions in $\mathscr{D}$. This decoupling has made it possible to find how different boundary conditions affect different types of turbulent flow in $\mathscr{E}$, as in the examples given above.

Class III. *Initial conditions and changing boundary conditions*

In turbulence with closed domains and deterministic boundary conditions (I) and with open domains and statistical boundary conditions (II), the turbulence in $\mathscr{D}$ is determined by boundary conditions (e.g. $\overline{M_m}^{(\mathscr{B})}$) near the bounding surface $\mathscr{B}$. These boundary conditions are assumed to persist for long enough, or not to change rapidly, so that the initial conditions of turbulence at $t = 0$ or the rate of change of its structure, do not have to be considered. In other words we ignore the dependence on $\overline{M_l}^{(0)}$. However, another class of problems specifically concerns how turbulence changes over a time, say $T_{\mathscr{D}}$, in different flows, given initial boundary conditions $\overline{M_l}^{(0)}$. We classify this as the third kind of problem. The flow domain in question may be closed or open, and may or may not have a mean flow across $\mathscr{B}$.

In many theoretical studies of the distortion of turbulent flows, in any of these three classes, it is convenient to consider first of all a well-posed mathematical problem of the time evolution of turbulent flows, with various different properties, under the action of different kinds of distortion, e.g. gradients of the mean velocity, a boundary being imposed or moved, the effect of a density gradient, etc. Then the results of the analysis, or computation, or experiment, can be applied to understanding or calculating the steady-flow problems of Class I or II. Usually this application is not exact, and involves heuristic approximations. But in some cases there is a formal mathematical connection, mainly between the flows of Classes III and II.2.1.

The time evolution problem can be analysed formally by RDT over a time period $T_{\mathscr{D}}$ which is less than the turbulence timescale T_{L}. For a longer period, approximations to RDT, or other methods, have to be used.

2.2. *Methods of solution*

Most turbulence problems would be regarded as solved when the functional relationship is known between the ensemble average of the kth-order multi-point moments of the velocity $\overline{M_k}$, in the flow domain $\mathscr{D}$, and the lth- and mth-order ensemble average moments of the velocity field on the boundary and at some initial moment. The methods that have been developed for obtaining such solutions can be divided into two distinct classes, which involve quite different equations, approximations and boundary conditions. The first class involves computational methods and approximations that are also used in studies of non-turbulent fluid flows, whereas the methods in the second of the classes are particular to turbulent flows and depend in large part on the assumption that turbulent flows have a common 'structure', a question we examine in detail in §§4 and 5.

2.2.1. *Modelling each realization* First the unsteady equations are approximated, for example, by discretization (as in direct numerical simulation), by filtering and discretization (as in large-eddy simulations), or by linearizations (as in rapid distortion theory).

Second, the approximate equations are solved subject to the boundary conditions at each realization. (In the case of RDT this step may be analytical.)

Third, using the solution for the ensemble of realizations the kth-order multipoint-time moments are computed or calculated. (In the case of RDT these can sometimes be calculated analytically.)

Where the results are computed directly, large numbers of realizations (typically 100) have to be computed to obtain even second-order, two-point moments. If the mean flow is steady, the moments can be derived from averages over time, and so computations should extend over many integral timescales (L_x/u_0); the higher the order of moments to be computed, the longer is the time required.

2.2.2. *Modelling ensembles of realizations* Quite different approximate procedures have been developed for use in practical calculations of turbulent flows, where mostly only first and second moments of the velocity field at one point are required. The solutions to the partial differential equations resulting from these methods usually require extensive and careful computation.

First the equation for kth-order moments (one-point or multi-point) are derived without approximation from the Navier–Stokes equation, and then the ensemble averages of the equations are taken (usually after separating the velocity field into mean, $\boldsymbol{U}(\boldsymbol{x},t)$, and fluctuating $\boldsymbol{u}(\boldsymbol{x},t)$, components).

There is no rigorous procedure for using this infinite set of equations to solve for

$M^{(k)}$, because the sequence of equations may not converge. These equations have to be approximated to be useful and to obtain a computationally soluble closed system of equations. The practitioners of approximate methods in turbulence have slowly converged onto the use of a few standard methods, ranging from the simplest, involving no extra equations (such as mixing length), to second- and third-order models involving ten or more extra equations. For inhomogeneous flows, one-point moments are reviewed by Launder & Spalding (1972) and Lumley (1978). For homogeneous turbulence, model equations for two-point, second- and third-order moments and spectra have been developed for isotropic and non-isotropic turbulence by methods ranging from the most fundamental, such as Kraichnan's DIA (based on truncating formal expansions: see Leslie 1973) to those based on physical assumptions about third- and fourth-order correlations such as the 'eddy damped quasi-normal Markovian' approximation, Lesieur 1987).

The various approximations used in the practical one-point models would, in principle, only be valid in all turbulent flows if they all had a similar 'structure' (for example in the relation between $\overline{u_i u_j}$ and $\overline{u_l u_l}$). In fact, many features of the turbulence structure are different, e.g. in the form of their spectra, yet these models, which all incorporate empirical coefficients, can be used approximately in a wide variety of complex, inhomogeneous turbulent flows (provided the models are used in the way they are designed to be used; e.g. the lowest-order models are essentially designed for computing the mean flow and not the turbulence structure). Some reasons for this approximate success are discussed in later sections.

These approximate moment equations can be solved only if suitable boundary conditions exist for the moments. If the equations are to be solved for turbulent flows at high Reynolds number, then boundary conditions (e.g. at a rigid surface $z = 0$), are required for all the moments of the derivatives as $z/L_x \to 0$, where L_x is a relevant scale of motion of the turbulence (e.g. an integral scale for one-point moments or distance between points in two-point moments).

Recent computational and experimental research has shown how the decreasing magnitude of certain lengthscales of turbulence at a rigid surface mean that the turbulence develops its own local structure at a rigid surface. In this limit, where the dynamics lead to a local structure, it is found that there are universal boundary conditions for second moments of the turbulence. (Townsend 1961 used this approach to show how the logarithmic law of the wall could be derived from the turbulent energy equation.)

Where the Reynolds number is too low, or the locally generated turbulence does not dominate the local structure (as, for example, in separated flow at a surface downwind of a fence, Ruderich & Fernholz 1986) there is no universal local structure. However, to obtain solutions to the moment equations, various approximate and empirical boundary conditions have been proposed for the moments of the velocity and their derivatives; these have to ensure that the no-slip conditions are satisfied and that the set of momentum equations can be solved efficiently and uniquely! (e.g. Rodi 1988). The detailed testing of these models, using direct numerical simulations (reviewed by Hunt 1988) is helping to establish whether and how these methods of solution can be used reliably near all surfaces. This is necessary since it appears that turbulence does not have a universal structure for different flows over the same kind of surface (as in the case of separated flows or where the turbulence is driven by body forces).

3. Mathematical developments of RDT

3.1. *Linearization*

Consider the random velocity pressure and vorticity fields $\boldsymbol{u}^*(\boldsymbol{x},t), p^*(\boldsymbol{x},t)\,\boldsymbol{\omega}^*(\boldsymbol{x},t)$ divided into the ensemble mean and fluctuating components, $\boldsymbol{u}^* = \boldsymbol{U}(\boldsymbol{x},t)+\boldsymbol{u}$, $p^* = \rho(P+p)$ and $\boldsymbol{\omega}^* = \boldsymbol{\Omega}+\boldsymbol{\omega}$. The ensemble means of $\boldsymbol{u}, p$ and $\boldsymbol{\omega}$ are zero. We now review the estimation of the errors associated with linearization, both for the large energy-containing scales of the turbulence with a typical r.m.s. velocity $u_0 = (\frac{1}{3}\overline{u_i u_i})^{\frac{1}{2}}$, and integral scale L_x, and for small eddies with velocity scale $u(l)$ and lengthscale l. The typical values of the mean velocity, and its change over a typical lengthscale of the mean flow in $\mathscr{D}$, are U_0 and ΔU_0 respectively.

In this paper the discussion of RDT is restricted to incompressible flows with uniform density and no body forces. But in fact RDT is a useful and easy technique for estimating how such effects change turbulent flows (e.g. Moffatt 1967; Komori *et al.* 1983).

The governing equations for $\boldsymbol{u}$ and $\boldsymbol{\omega}$ are

$$\frac{\partial u_i}{\partial t}+U_j\frac{\partial u_i}{\partial x_j}+u_j\frac{\partial U_i}{\partial x_j}-=-\frac{\partial p}{\partial x_i}+\nu\nabla^2 u_i-(\mathrm{NL})_{u_i}, \tag{3.1a}$$

$$\frac{\partial \omega_i}{\partial t}+\underbrace{U_j\frac{\partial \omega_i}{\partial x_j}}_{\text{(i)}}+\underbrace{u_k\frac{\partial \Omega_i}{\partial x_k}}_{\text{(ii)}}-\underbrace{\omega_k\frac{\partial U_i}{\partial x_n}}_{\text{(iii)}}-\underbrace{\Omega_n\frac{\partial u_i}{\partial x_n}}_{\text{(iv)}}=\nu\nabla^2\omega_i+(\mathrm{NL})_{\Omega_i}, \tag{3.1b}$$

where
$$\partial u_i/\partial x_i = 0, \quad \omega_i = \epsilon_{ijk}\,\partial u_k/\partial x_j, \tag{3.1c}$$

so that $\partial\omega_k/\partial x_k = 0$.

The physical interpretation of the terms in (3.1*b*) has been given by various authors (e.g. Tennekes & Lumley 1971; Hunt 1978). The terms (i) and (iii) for the advection and stretching of $\boldsymbol{\omega}$ by the mean flow are important in all flows with a mean velocity. The fourth term (iv) is significant where the mean vorticity exists and can be distorted by velocity fluctuations. The second term (ii) caused by the advection of the mean vorticity by the turbulence is only significant if the mean vorticity is non-uniform (Gartshore, Durbin & Hunt 1983).

The nonlinear terms are

in (3.1*a*)
$$(\mathrm{NL})_{u_i} = -\left[\frac{\partial(u_k u_i)}{\partial x_k}-\frac{\partial\overline{u_k u_i}}{\partial x_k}\right], \tag{3.2a}$$

and (3.1*b*)
$$(\mathrm{NL})_{\Omega_i} = -u_k\frac{\partial\omega_i}{\partial x_k}+\omega_j\frac{\partial u_i}{\partial x_j}+\overline{\frac{u_k\,\partial\omega_i}{\partial x_k}}-\overline{\frac{\omega_j\,\partial u_i}{\partial x_j}}. \tag{3.2b}$$

The first term is advection of $\boldsymbol{\omega}$ by the fluctuating vorticity and the second is the stretching of $\boldsymbol{\omega}$ by the fluctuating velocity.

In RDT the linearized velocity and/or vorticity equations (3.1) are primarily used to calculate the two-point moment of the velocity field, $R_{ij}(\boldsymbol{r}) = \overline{u_i(\boldsymbol{x})\,u_j(\boldsymbol{x},\boldsymbol{r})}$, or the two-point structure function such as $\Delta R_{ii}(\boldsymbol{x},\boldsymbol{r}) = \overline{(u_i(\boldsymbol{x})-u_i(\boldsymbol{x},\boldsymbol{r})^2} = 2(\overline{u_i^2}-R_{ii}(\boldsymbol{x},\boldsymbol{r}))$. The conditions for linearization of (3.1*b*) are quite different if $\boldsymbol{\omega}$ is calculated for the purpose of calculating $\boldsymbol{u}$ and R_{ii}, as compared with calculating $\overline{\omega_i^2}$. It is necessary to define which scale of the vorticity field contributes to the moments of the velocity field.

Using the Biot–Savart integral (Batchelor 1967, chap. 2), $\Delta R_{ii}(\boldsymbol{x},\boldsymbol{r})$ can be

expressed as an integral of $\overline{\omega_k(\boldsymbol{r}')\,\omega_l(\boldsymbol{r}'')}$ which, for high-Reynolds-number turbulence, can be estimated in terms of the rate of dissipation per unit mass, ϵ. When

$$|(\boldsymbol{r}'-\boldsymbol{r}'')| < L_x,\ \overline{\omega_k(\boldsymbol{r}')\,\omega_l(\boldsymbol{r}'')} \sim \epsilon^{\frac{2}{3}}\hat{r}^{-\frac{4}{3}},$$

where $\hat{r} = |(\boldsymbol{r}'-\boldsymbol{r}'')|$, and thence, if $|\boldsymbol{r}| = l$,

$$\Delta R_{ii}(\boldsymbol{x},\boldsymbol{r}) \sim \int_0^l \epsilon^{\frac{2}{3}}\hat{r}^{-\frac{4}{3}}\hat{r}\,\mathrm{d}\hat{r} \sim \epsilon^{\frac{2}{3}}l^{\frac{2}{3}}. \tag{3.3}$$

This integral shows that, although the vorticity correlation is largest at very small separations of $\hat{\boldsymbol{r}}$, the contribution to ΔR_{ii} from smaller-scale vorticity is comparable with that from lengthscales of the vorticity centred on l.

The contributions to eddies on scale l or $\Delta R_{ii}(l)$ from vorticity of different lengthscales could come from vortex sheets separated by L_x or from smooth distributions of vorticity on a scale l, or from both. Flow visualizations and measurements using conditional sampling (e.g. Hussain 1986), the analyses of Moffatt (1984) and Gilbert (1988), and the numerical simulations of two-dimensional high-Reynolds-number vortices by Dritschel (1989) suggest that both forms exist simultaneously because each type of vorticity distribution eventually develops into the other type. However, it does appear that velocity fluctuations on a scale l are primarily associated with smoothly distributed vorticity regions with lengthscale l, so that nonlinear terms like $\omega_j\,\partial u_i/\partial x_j$ can be estimated as being of order $u^2(l)/l^2$. Of course if (3.1*b*) was used to compute the mean-square vorticity, the nonlinear terms would be of order $\overline{\omega^2}$ and greater by a factor of $O(\overline{w^2}l^2/u^2) = O(Re)$ if $l \sim L$ (Tennekes & Lumley 1971).

The effect of the nonlinear terms in (3.1*b*) not only has to be estimated over the appropriate lengthscale of the velocity field (l), but also over the period $T_{\mathscr{D}}$ in which the mean distortion is applied. Since these terms are randomly varying in time and space, their effect is reduced. The second of the nonlinear terms in (3.2*b*) is caused by the stretching of the fluctuating vorticity $\boldsymbol{\omega}$ by the fluctuating velocity, $\boldsymbol{u}$, and can be estimated for high-Reynolds-number turbulence, using the fact that, on a lengthscale l, $\partial u_i/\partial x_j$ is of order $\epsilon^{\frac{1}{3}}l^{-\frac{2}{3}}$. Now we can estimate the relative changes in ω produced, in a time $T_{\mathscr{D}}$, by the linear ($\Delta\omega_{\mathrm{Lin}}$) and nonlinear terms ($\Delta\omega_{\mathrm{NL}}$) compared with the initial vorticity (ω_0). Thus $\Delta\omega_{\mathrm{Lin}}/\omega_0 \sim (\Delta U/L_{\mathscr{D}})\,T_{\mathscr{D}}$, $\Delta\omega_{\mathrm{NL}}/\omega_0 \sim (u(l)/l)\,T_{\mathscr{D}}$. Therefore, for the purposes of estimating moments of $u(l)$ on a scale l, the criterion for neglecting the nonlinear vortex stretching term $\omega_j\,\partial u_i/\partial x_j$ is

$$\frac{u(l)}{l} \sim \epsilon^{\frac{1}{3}}l^{-\frac{2}{3}} \ll \max\left(\frac{\Delta U}{L_{\mathscr{D}}}, \frac{1}{T_{\mathscr{D}}}\right). \tag{3.4}$$

This criterion can also be expressed in terms of the characteristic velocity of the energy-containing eddies u_0. Since, from the inertial-range scaling $u(l) \sim u_0(l/L_x)^{\frac{1}{3}}$, (3.4) becomes

$$\frac{u_0}{L_x}\left(\frac{l}{L_x}\right)^{-\frac{2}{3}} \ll \max\left(\frac{\Delta U}{L_{\mathscr{D}}}, \frac{1}{T_{\mathscr{D}}}\right). \tag{3.5}$$

Thus the two dimensionless parameters which characterize the energy-containing eddies ($l \sim L_x$) of a rapidly distorted flow are: the total strain $\beta = T_{\mathscr{D}}\Delta U/L_{\mathscr{D}}$ and the relative strain rate

$$\mathscr{S}^* = (\Delta U/L_{\mathscr{D}})\,T_{\mathrm{L}} \quad \text{where } T_{\mathrm{L}} = L_x/u_0. \tag{3.6}$$

The criterion of (3.5) implies that, if the strain rate is weak, i.e. $\mathscr{S}^* \leqslant 1$,

$$(\beta/\mathscr{S}^*) \ll 1, \quad \text{or} \quad T_{\mathscr{D}} \ll T_{\mathrm{L}}. \tag{3.7a}$$

But if the strain rate is strong, $\mathscr{S}^* \gg 1$, then

$$\beta/\mathscr{S}^* \text{ or } T_{\mathscr{D}}/T_{\mathrm{L}} \text{ are arbitrary} \tag{3.7b}$$

(see Lee *et al.* 1988). If (3.5) is satisfied the effects of random straining with large timescales are also negligible. Equation (3.5) is the essential criterion for the validity of RDT calculations of second moments of the velocity field for rapidly changing turbulent flow (RCT): it indicates that the linearization is justifiable either if the strain rate is large enough or if the period of distortion T_{D} is short enough. It also shows that the neglect of nonlinear processes for the energy-containing eddies (where $l \sim L_x$) is better justified than for smaller-scale eddies (where $l \ll L_x$). (For low Reynolds number turbulence this caveat is not necessary.) Usually the mean straining motion selectively amplifies the turbulent vorticity $\boldsymbol{\omega}$ in one or two directions, and may even reduce $\boldsymbol{\omega}$ in other directions. Therefore (3.7*a*, *b*) are the criteria for the linear analysis to describe the growth of the components of vorticity and velocity with maximum magnitudes.

In deriving (3.5) only the nonlinear random stretching is considered, which in some cases can amplify the anistropy of $\boldsymbol{\omega}$ produced by the linear distortion (Lee 1985; Kida & Hunt 1989). However, an important effect of the nonlinear terms is the random rotation of vortex lines by the turbulence, leading to significant transfer of vorticity into directions away from those of maximum straining. Thus, linear analysis can under- or overestimate the anisotropy caused by mean strain. Therefore the criterion (3.5) for the neglect of nonlinear terms can only be applied to all vorticity and velocity components if it is modified to allow for the reduced straining in some directions and the nonlinear rotation effect. So (3.5) becomes

$$\frac{u_0}{L_x}\left(\frac{l}{L_x}\right)^{-\frac{2}{3}} \ll \max\left(\frac{\Delta U}{L_{\mathscr{D}}}\theta(T_{\mathscr{D}}), \frac{1}{T_{\mathscr{D}}}\right), \tag{3.8}$$

where $\theta(T_{\mathscr{D}}) = \exp((\lambda_{\min} - \lambda_{\max})T_{\mathscr{D}})$, and $\lambda_{\max}$ and $\lambda_{\min}$ are the moduli of the maximum and minimum values of principal strains of $\partial U_i/\partial x_j$. This means that the strain parameter criterion (3.7*b*) is changed to

$$\mathscr{S}^*\theta \gg 1. \tag{3.9}$$

So for strong enough isotropic compressive strains, where $\partial U_i/\partial x_j \propto \delta_{ij}$ and $\theta = 1$, and if (3.7*b*) is satisfied, the nonlinear terms can be neglected for all time (Batchelor 1955). If, for any non-isotropic strain, the effective angle of rotation $\theta(T_{\mathscr{D}})$ increases with time, then the nonlinear terms eventually become significant, whatever the initial strength of the strain. (We return to this in §4.)

3.2. *The statistical input and output to RDT*

It is not possible in general to calculate, even using linear RDT, the changes of $\boldsymbol{u}$ or $\boldsymbol{\omega}$ over the domain $\mathscr{D}$ for an arbitrary input distribution $\boldsymbol{u}_0(\boldsymbol{x}, t)$ whether it is defined initially and/or over the boundary $\mathscr{B}$. But, by representing u_{0i} as a series, or integrals of orthogonal functions $\phi_{0i}^{(n)}$, where the random coefficients $S_{0i}^{(n)}$ are defined by the input distribution, it is possible to calculate the changes in $\mathscr{D}$ of $\boldsymbol{u}(\boldsymbol{x}, t)$ (and its moments) for a wide range of statistical distributions of $\boldsymbol{u}_0$.

In general

$$u_{0i}(\boldsymbol{x}, t) = \sum S_{0i}^{(n)} \phi_{0i}^{(n)}(\boldsymbol{x}, t), \tag{3.10}$$

where the orthogonal functions $\phi_{0i}^{(n)}(\boldsymbol{x}, t)$ can, in principle, be deduced from (laborious) measurements or computations of two-point moment of u_{0i} (Lumley 1965).

When the 'input' velocity field is homogeneous, Fourier integrals are used in place of the sum (3.10) and the functions $\phi_0(\boldsymbol{x})$ are known, so that

$$u_{0i}(\boldsymbol{x},t) = \int S_{0i}(\boldsymbol{\kappa},t)\,\mathrm{e}^{\mathrm{i}\boldsymbol{\kappa}\cdot\boldsymbol{x}}\,\mathrm{d}\boldsymbol{\kappa}. \tag{3.11a}$$

The correlations between these random Fourier transforms S_{0i} are defined by the orthogonality relation

$$\overline{S^*_{0i}(\boldsymbol{\kappa})\,S_{0j}(\boldsymbol{\kappa}')} = \delta(\boldsymbol{\kappa}-\boldsymbol{\kappa}')\,\Phi_{0ij}(\boldsymbol{\kappa}), \tag{3.11b}$$

where $\Phi_{0ij}(\boldsymbol{\kappa})$ is the energy spectrum tensor, and

$$\frac{1}{(2\pi)^3}\int R_{0ij}(\boldsymbol{x},\boldsymbol{x}+\boldsymbol{r})\,\mathrm{e}^{-\mathrm{i}\boldsymbol{\kappa}\cdot\boldsymbol{r}}\,\mathrm{d}\boldsymbol{r} = \Phi_{0ij}(\boldsymbol{\kappa}). \tag{3.11c}$$

Changes to u_i can be expressed as the product of a non-random 'transfer function' $Q_{ik}(\boldsymbol{\kappa},\boldsymbol{x},t)$ and the original Fourier transform

$$u_i(\boldsymbol{x},t) = \int_{\boldsymbol{\kappa}} Q_{ij}(\boldsymbol{\kappa},\boldsymbol{x},t)\,S_{0j}(\boldsymbol{\kappa},t)\,\mathrm{d}\boldsymbol{\kappa}, \tag{3.12a}$$

where at $t=0$, $Q_{ij} = \delta_{ij}\,\mathrm{e}^{\mathrm{i}\boldsymbol{\kappa}\cdot\boldsymbol{x}}$, but for $t>0$, Q_{ij} is determined by the dynamical equations. Similar transfer functions can be defined for pressure, Π_m, in terms of the initial velocity S_{0j}, and for vorticity, q_{im}, in terms of the Fourier transform of the initial vorticity. Note that S_{0j}, Q_{ij} and q_{im} are related by

$$\epsilon_{ijk}\frac{\partial Q_{kr}}{\partial x_j} = \mathrm{i}q_{in}\,\epsilon_{npr}\,k_p. \tag{3.12b}$$

From (3.11) and (3.12) the changed two-point moments are determined by the transfer functions and the original spectrum:

$$R_{ij}(\boldsymbol{x},\boldsymbol{x}+\boldsymbol{r}) = \int_{\boldsymbol{k}} Q^*_{im}\,Q_{jl}\,\Phi_{0ml}\,\mathrm{d}\boldsymbol{\kappa}. \tag{3.13}$$

All the other one- and two-point second moments and spectra can be derived from (3.13) (e.g. Hunt 1973).

In most computations of rapid distortion theory, it has been assumed that the input turbulence is isotropic (and incompressible), so that $\Phi_{0ij}(\boldsymbol{\kappa})$ could be expressed simply and uniquely as

$$\Phi_{0ij} = \frac{E(k)}{4\pi}(k^2\delta_{ij}-\kappa_i\kappa_j), \tag{3.14a}$$

where $k^2 = \kappa_i\kappa_i$ and $E(k)$ is the energy spectrum, whose integral is

$$\int_0^\infty E(k)\,\mathrm{d}k = \tfrac{1}{2}u_i\,u_i. \tag{3.14b}$$

To investigate how distorted homogeneous turbulence depends on its initial conditions, either the spectrum $E(k)$ or the anisotropy are varied. For axisymmetric turbulence, Φ_{0ij} is defined by Batchelor (1953); for isotropic turbulence in two-dimensions, (3.14) can be applied to two dimensions only. In axisymmetric turbulence

$$\Phi_{0ij} = I_{ij}B_1(k,\boldsymbol{\kappa}\cdot\boldsymbol{e}) + H_{ij}B_2(k,\boldsymbol{\kappa}\cdot\boldsymbol{e}),$$

where

$$I_{ij} = \delta_{ij}-\frac{\kappa_i\kappa_j}{k^2}, \quad H_{ij} = e_ie_j+\frac{(\kappa_k e_k)^2}{k^2}\delta_{ij}-\frac{\kappa_k e_k(e_i\kappa_j+e_j\kappa_i)}{k^2}. \tag{3.15}$$

As a simple hypothesis it is usually further assumed that B_2 is zero and B_1 is a function of k only (Sreenivasan & Narasimha 1978; Maxey 1982).

Note that where the initial state of the turbulence is assumed to be homogeneous, the general representation (3.13) does not necessarily imply that the turbulence remains homogeneous while being distorted. In many studies of RDT from Batchelor & Proudman (1954) onwards, it has been assumed that the turbulence remains homogeneous during the distortion. In that case the transfer functions Q_{in} and q_{in} can be expressed (in a suitable moving frame) as

$$\{Q_{in}(\boldsymbol{\kappa};\boldsymbol{x},t), q_{ip}(\boldsymbol{\kappa};\boldsymbol{x},t), \Pi_n(\boldsymbol{\kappa};\boldsymbol{x},t)\} = \{A_{in}(\boldsymbol{\chi},t), a_{ip}(\boldsymbol{\chi},t), \hat{P}_n(\boldsymbol{\chi},t)\}\,\mathrm{e}^{\mathrm{i}\chi\cdot x}, \quad (3.16a)$$

where

$$a_{ip} = -\epsilon_{ijk}\,\epsilon_{nmp}\,k_m\,\chi_j A_{kn}/k^2 \quad (3.16b)$$

and $\boldsymbol{\chi}$ is the local deformed wavenumber defined by the constraint that wave fronts are conserved, i.e.

$$\mathrm{d}\chi_l/\mathrm{d}t + \chi_l\,\partial U_l/\partial x_i = 0, \quad (3.16c)$$

$\mathrm{d}/\mathrm{d}t$ being evaluated in the moving frame, and $\boldsymbol{\chi}(t=0) = \boldsymbol{\kappa}$. In these homogeneous distortions, a local energy spectrum tensor can be derived from the transfer function, viz.

$$\Phi_{ij}(\boldsymbol{x}) = A^*_{in} A_{jm}(\boldsymbol{\chi},t)\,\Phi_{0nm}(\boldsymbol{\kappa}). \quad (3.17)$$

In many cases the turbulence is homogeneous in only one direction (say x_3) and in time, and then (3.16) can be generalized (following Phillips 1955 and Hunt 1973) to

$$Q_{in}(\boldsymbol{\kappa};\boldsymbol{x},t) = M_{in}(\boldsymbol{\chi};x_1,x_2)\,\mathrm{e}^{\mathrm{i}(\chi_3 x_3+\omega t)} \quad (3.18)$$

where

$$\mathrm{d}\chi_3/\mathrm{d}t + \chi_3\,\partial U_3/\partial x_3 = 0.$$

In this case spectra can be defined for wavenumber χ_3 or frequency ω.

3.3. *Methods of solution*

The essential point about RDT is that it is a method for calculating what happens to an initial velocity distribution using the linearized equations of motion under particular kinds of distortion, such as occur in the boundary-value problems classified in §2 as II.1 and III. In some cases, RDT provides a practical method of calculating turbulent flows at the appropriate level of moments (e.g. second order, two point) and appropriate accuracy. It is not a method of explaining how any turbulent flow arises, nor in general, a method of calculating the flow everywhere in a flow domain. However, it can be used as a diagnostic tool for studying certain aspects of the mechanics of turbulent flows. Many different kinds of distortion and initial condition have been used in a wide range of practical and fundamental studies. Different methods of solution can usefully be classified according to whether the distortions are homogeneous or inhomogeneous.

3.3.1 *Homogeneous distortion (without body forces)* In this case the turbulent velocity and vorticity fields are homogeneous and can be represented by a three-dimensional Fourier transform throughout the distortion, as described by (3.16). This form of solution is appropriate if the rate of strain of the mean velocity field $\partial U_i/\partial x_k$ is uniform, so that the mean velocity can be expressed as $U_i = x_j \alpha_{ij}$.

(i) Using the linearized vorticity equation (3.1*b*) and substituting (3.16*a*) and (3.16*b*) leads to

$$\frac{\mathrm{d}a_{in}}{\mathrm{d}t} = a_{jn}\frac{\partial U_i}{\partial x_j} + \mathrm{i}\Omega_j\chi_j A_{in}, \quad (3.19)$$

which reduces to an equation for the vorticity tensor:

$$\frac{\mathrm{d}a_{in}}{\mathrm{d}t} = \beta_{ik}a_{kn}. \quad \text{where} \quad \beta_{ik} = \alpha_{ik} - \epsilon_{ijk}\epsilon_{lmn}\alpha_{nm}\chi_l\chi_j/\chi^2, \qquad (3.20a, b)$$

and χ_l is given by (3.16*c*). In general $\partial U_i/\partial x_k$ and $\Omega_l = \epsilon_{lmn}\partial U_n/\partial x_m$ are specified as functions of time. Also at $t = 0$, $a_{in} = \delta_{in}$.

For irrotational mean flows, where $\Omega_l = 0$, β_{ik} is independent of the wavenumber vector χ_l, and the change in $a_{in}(t)$ depends solely on the integral of the strain rate $\int(\partial U_i/\partial x_k)\,\mathrm{d}t$. Also in this case the vorticity tensor $\beta_{ik} = \alpha_{ik}$, which is just the negative of the tensor given by (3.16*c*) for the rate of change of the wavenumber i.e. $-\alpha_{ki} = -\alpha_{ik}$. But for rotational mean flows, the change in a_{in} is dependent on the wavenumber and on the history of the changes in $\partial U_i/\partial x_k$. There is no simple relation between β_{ik} and how χ_i changes. Specific examples of sequences of irrotational and rotational strains were calculated by Townsend (1980), and Sreenivasan (1985).

Unique solutions for a_{in}, and thence A_{in} and χ_i can be expressed as

$$a_{in}(\boldsymbol{\chi}, t) = T_{ij}(t)\,a_{jn}(\boldsymbol{\kappa}, 0), \quad \chi_i = \kappa_j S_{ji},$$

where the deformation tensors T_{ij}, S_{ji} can be formally expressed as integrals of the $\beta_{ik}(t)$ and $\alpha_{ij}(t)$ (e.g. Kida & Hunt 1989).

Once A_{in} and χ_i are found, the new three-dimensional spectra and cross-correlations can be derived from (3.12) and (3.16). Usually (3.20*b*) is only used for irrotational distortions, but it has been used for combinations of irrotational and rotational distortions by Kida & Hunt (1989).

(ii) The alternative approach (developed by Craya 1958; Deissler 1968 and Townsend 1976) to the calculation of the transfer function is to use the linearized momentum equations directly. For a locally homogeneous solution, the transfer function A_{in} satisfies

$$\frac{\mathrm{d}}{\mathrm{d}t}A_{in} = -A_{jn}\alpha_{ij} - i\chi_i\hat{p}_n. \qquad (3.21a)$$

Using continuity, $\chi_j A_{jn} = 0$, and (3.16*c*) for the change of χ_j, $\hat{p}_n$ can be expressed in terms of A_{in} as

$$\hat{p}_n = \mathrm{i}[\chi_i A_{jn}\alpha_{ij} - A_{in}\,\mathrm{d}\chi_i/\mathrm{d}t]/\chi^2. \qquad (3.21b)$$

Therefore $\mathrm{d}A_{in}/\mathrm{d}t = \mu_{ik}A_{kn}$, where

$$\mu_{ik} = -[\alpha_{ik} - 2\chi_i\chi_j\alpha_{jk}/\chi^2] \quad \text{and} \quad A_{kn}(t = 0) = \delta_{kn}. \qquad (3.22)$$

This solution shows how, even in this linear theory the pressure gradient generates fluctuating motions in directions perpendicular to the mean velocity $\boldsymbol{U}$ of the straining motion, and tends to reduce the motion in the direction of mean strain. From (3.22) A_{in} can be defined explicitly for weak distortion, i.e. $t\|\boldsymbol{\nabla U}\| \ll 1$, (Crow 1968) viz.

$$A_{in}(t) = (\delta_{ik} + t\mu_{ik}(t = 0))\,\delta_{kn}. \qquad (3.23)$$

Even for finite distortions, the equations can be integrated analytically in cases where α_{ik} is constant in time. Simple results are available for pure shear, pure rotation, and irrotational distortion (e.g. Townsend 1970; Cambon & Jacquin 1989).

3.2.3. *Inhomogeneous distortions* Now consider the theory when the integral lengthscale of the initial homogeneous turbulence L_x is comparable with the lengthscale $L_{\mathscr{D}}$ over which the mean velocity gradients ($\boldsymbol{\nabla U}$) vary, or comparable

with the distance n to a boundary which makes the turbulence inhomogeneous (such as a density discontinuity or a boundary with another kind of velocity field), i.e.

$$L_x > L_{\mathscr{D}} \sim \|\nabla U\|/\|\nabla\nabla U\| \quad \text{or} \quad L_x > n.$$

New solutions have to be found for the velocity, vorticity and pressure transfer functions $(Q_{in}, q_{in}, \Pi_n)(\boldsymbol{\kappa}, \boldsymbol{x}, t)$. So far general methods have been found for *irrotational flows*, but for *rotational* mean flows where the turbulence is inhomogeneous, solutions have been found only for a few classes of mean flow, initial turbulence and boundary conditions. A feature of all inhomogeneous problems is that the boundary and initial conditions have a significant effect on the solution and have to be carefully specified.

Irrotational mean flow. In these problems the distortion of a weak random vorticity field by a strong irrotational mean straining flow is calculated. There may also be a significant (not necessarily weak) irrotational fluctuating velocity field.

(*a*) *The vorticity method* Since the mean vorticity is zero, i.e. $\boldsymbol{\Omega} = \nabla \wedge \boldsymbol{U} = 0$, the linearized vorticity equation (3.1*b*) reduces to

$$\partial\boldsymbol{\omega}/\partial t + (\boldsymbol{U}\cdot\nabla)\,\boldsymbol{\omega} = (\boldsymbol{\omega}\cdot\nabla)\,\boldsymbol{U}, \tag{3.24}$$

and $\boldsymbol{u}$ can be solved from $\boldsymbol{\omega} = \nabla \wedge \boldsymbol{u}$ and $\nabla\cdot\boldsymbol{u} = 0$.

For the solution for the fluctuating vorticity field in the flow domain $\mathscr{D}$, the only boundary conditions required are its initial vorticity $\boldsymbol{\omega}_0(\boldsymbol{x}, t)$ at $t = t_0$, and its value on $\mathscr{B}$, $\boldsymbol{\omega}_{\mathscr{B}}(\boldsymbol{x}_{\mathscr{B}}, t)$, where the mean velocity is entering the flow domain, i.e. $\boldsymbol{U}\cdot\boldsymbol{n}_{\mathscr{B}} < 0$. The fluctuating velocity field is similarly specified:

$$\boldsymbol{u} = \boldsymbol{u}_0(\boldsymbol{x}, t_0) \tag{3.25a}$$

and

$$\boldsymbol{u} = \boldsymbol{u}_{\mathscr{B}}(\boldsymbol{x}, t) \quad \text{on} \quad \boldsymbol{x}_{\mathscr{B}} \tag{3.25b}$$

(where $\boldsymbol{u}_{\mathscr{B}}$ may be an implicit function of $\boldsymbol{u}$ in $\mathscr{D}$ and of $\boldsymbol{u}$ in $\mathscr{E}$ outside $\mathscr{B}$). Of course on a rigid bounding surface, $\mathscr{B}_S$,

$$\boldsymbol{u}_{\mathscr{B}}\cdot\boldsymbol{n} = 0 \quad \text{on} \quad \boldsymbol{x} = \boldsymbol{x}_{\mathscr{B}_S}. \tag{3.25c}$$

First $\boldsymbol{\omega}$ is solved in terms of its initial or boundary vorticity (both denoted here by $\boldsymbol{\omega}_0$) and the mean velocity field, using Cauchy's theorem. Let $\boldsymbol{x}$ be the position of a fluid element at time t and $\boldsymbol{a}(\boldsymbol{x})$ be its position earlier at time t_0 (or $t_{\mathscr{B}}$ if on $\mathscr{B}$) when it is first advected by the mean flow. By considering corresponding small changes in $\boldsymbol{x}$ and $\boldsymbol{a}$, which is equivalent to considering the distortions of a line element (Batchelor 1967, Chap. 6), it follows that the solution to (3.24) is

$$\omega_i(\boldsymbol{x}, t) = \omega_{0j}(\boldsymbol{a}, t_0)\,\partial x_i/\partial a_j. \tag{3.26a}$$

For two-dimensional and axisymmetric flows, the tensor $\partial x_i/\partial a_j$ can be derived explicitly in terms of derivatives of the stream function (or Stokes stream function) ψ and the drift function $T(\boldsymbol{x})$ or time of flight from a plane $x_i = X$ along a mean streamline $\psi = \text{const}$;

$$T_X(\boldsymbol{x}) = \int_X^{x_1} \frac{\mathrm{d}x'}{U_1(\boldsymbol{x}', t')} (\psi = \text{const})$$

(Hunt 1973; Durbin 1981).

Once $\boldsymbol{\omega}$ is solved, $\boldsymbol{u}$ can be calculated by standard kinematical methods (Batchelor 1967, Chap. 3; Hunt 1973). For a turbulent flow, it follows from (3.16*a*) and (3.26*a*) that the vorticity 'transfer function' is given simply by

$$q_{in}(\boldsymbol{\kappa}, \boldsymbol{x}, t) = (\partial x_i/\partial a_j)\,\delta_{jn}\,\mathrm{e}^{\mathrm{i}(\boldsymbol{\kappa}\cdot\boldsymbol{a})}, \tag{3.26b}$$

so that its distortion is independent of wavenumber. But the distortion of the velocity transfer function $Q_{in}(\boldsymbol{\kappa}, \boldsymbol{x}, t)$, which is derived from q_{in} using (3.12*b*) and a Biot–Savart integration, depends on the wavenumber $\boldsymbol{\kappa}$. Since Q_{in} also depends on the velocity boundary condition (3.25), it usually can only be derived analytically using asymptotic solutions, for very large or very small wavenumbers (i.e. $kL_{\mathscr{D}} \ll 1$ or $kL_{\mathscr{D}} \gg 1$). Thence velocity (and pressure) correlations can be calculated for small or large scales of turbulence relative to $L_{\mathscr{D}}$ (i.e. $L_x \ll L_{\mathscr{D}}$ or $L_x \gg L_{\mathscr{D}}$). For these limiting cases, the turbulence can be computed for quite complex flows, such as round circular cylinders, rectangular prisms, porous obstacles or spheres, etc. (Computations of the linear equation or Biot–Savart integrals are possible, in principle, for all $\boldsymbol{\kappa}$, but this approach has not yet been developed.)

A number of experiments performed to test these predictions have shown firstly that the changes in these limiting solutions as $L_x/L_{\mathscr{D}}$ changes are similar to the changes in the measured variances and correlations of the turbulence and the pressure fluctuations. Secondly, spectra measured at high and low wavenumbers correspond closely to the asymptotic limits (Graham 1976; Britter, Hunt & Mumford 1979; Durbin & Hunt 1980; Durbin 1981; Kawai 1989).

(*b*) *The velocity method* In an important development in RDT, Goldstein (1978) showed that in an irrotational distortion the velocity field $\boldsymbol{u}$ could be computed directly without the necessity of first computing the vorticity field. In his analysis he rediscovered Weber's (1868) result that the velocity of a fluid element at $\boldsymbol{x}$ at time t could be expressed as the sum of an irrotational component $\nabla\phi$ and a rotational component $\boldsymbol{u}_{\mathrm{R}}$ directly related to the velocity of the same element of $\boldsymbol{a}$ at time t_0, using the inverse of the same material deformation tensor as used for the change of vorticity, i.e.

$$u_i(\boldsymbol{x}, t) = u_{\mathrm{R}i} + \frac{\partial \phi}{\partial x_i}(\boldsymbol{x}, t), \quad \text{where} \quad u_{\mathrm{R}i}(\boldsymbol{x}, t) = \frac{\partial a_j}{\partial x_i} u_j(\boldsymbol{a}, t_0) \qquad (3.27a, b)$$

and $\phi(\boldsymbol{x}, t)$ is a velocity potential which is zero when $t = t_0$. To calculate ϕ it is only necessary to satisfy continuity ($\nabla \cdot \boldsymbol{u} = 0$) by solving one Poisson equation:

$$\nabla^2 \phi = -\nabla \cdot \boldsymbol{u}_{\mathrm{R}}, \qquad (3.27c)$$

subject to $(\boldsymbol{u}_{\mathrm{R}} + \nabla\phi)$ satisfying the boundary conditions (3.25). (By comparison the method (*a*) requires in principle four supplementary Poisson-type equations to be solved.)

The result (3.27) can be most easily understood by considering the change of $\boldsymbol{u} \cdot \mathrm{d}\boldsymbol{x}$ of a line element as it moves from $\boldsymbol{a}$ to $\boldsymbol{x}$, using Kelvin's theorem (Hunt 1987). Consequently (3.27) is also valid for barotropic, compressible flows.

This method was used to calculate the distortion of turbulence in a two-dimensional contracting duct (such as an aeroengine compressor duct) where the turbulence scale L_x is comparable with the scale of the duct, so that the eddies impact on its walls, as well as being strong distorted (Goldstein & Durbin 1980).

Rotational mean flow. An essential feature of RDT solutions for homogeneous or inhomogeneous flows is that no assumptions are made about the variation with time of the transfer function Q_{in} or q_{in} in $(\boldsymbol{\kappa}, \boldsymbol{x}, t)$. Therefore in some parts of the flow there may be amplification and in other parts reduction of different components of the turbulence velocity. This is quite unlike solutions of the linearized equations examined in hydrodynamic stability theory, where the time and space variations are decoupled and eigensolutions are calculated of the form

$$\boldsymbol{u}(\boldsymbol{x}, t) \propto \boldsymbol{f}(\boldsymbol{x})\, \mathrm{e}^{\mathrm{i}\sigma t}, \qquad (3.28)$$

where σ is a constant across the flow. The RDT solutions for inhomogeneous rotational straining motions are difficult to obtain analytically (for all wavenumbers) because the assumption (3.28) is not made, and because, when $\boldsymbol{\Omega} \neq 0$, the equation (3.1*b*) for fluctuating vorticity $\boldsymbol{\omega}$ also includes extra terms in the velocity, viz. $(\boldsymbol{\Omega}\cdot\nabla)\boldsymbol{u}$ and $-(\boldsymbol{u}\cdot\nabla)\boldsymbol{\Omega}$.

Interesting solutions have been obtained for inhomogeneous turbulence in various kinds of unidirectional shear flows. In the first case, consider a uniform shear flow $\boldsymbol{U}$ over a rigid flat boundary parallel to the mean flow, where

$$\boldsymbol{U} = (U_0 + \alpha x_2, 0, 0), \quad x_2 > 0, \tag{3.29a}$$

the turbulent vorticity $\boldsymbol{\omega}_0$ is initially homogeneous at $t = 0$, and there is no motion across the boundary, so

$$u_2 = 0 \quad \text{on} \quad x_2 = 0, \quad t > 0 \tag{3.29b}$$

(Maxey 1978; Lee & Hunt 1989). In a uniform shear the equations yield an explicit equation for $u_2(\boldsymbol{x}, t)$, namely

$$\left(\frac{\partial}{\partial t} + U_1 \frac{\partial}{\partial x_1}\right) \nabla^2 u_2 = 0. \tag{3.30}$$

Therefore a solution can be constructed in the form

$$u_2 = u_2^{(\mathrm{H})}(\boldsymbol{x}, t) + \partial\phi/\partial x_2, \tag{3.31a}$$

where $u_2^{(\mathrm{H})}$ is a homogeneous solution such that

$$\nabla^2 u_2^{(\mathrm{H})} = \nabla^2 u_2^{(\mathrm{H})}(\boldsymbol{x}, t = 0) \quad \text{and} \quad \nabla^2\phi = 0. \tag{3.31b, c}$$

Thence using (3.18) and (3.31) the 'transfer function' for u_2 can be expressed as

$$Q_{2n} = A_{2n}(\boldsymbol{\chi}, t)\, \mathrm{e}^{\mathrm{i}(\boldsymbol{\kappa}\cdot\boldsymbol{x})} + \frac{\partial\hat{\phi}_n}{\partial x_2}(\boldsymbol{\kappa}_{13}, y; t)\, \mathrm{e}^{\mathrm{i}(\boldsymbol{\kappa}_{13}\cdot\boldsymbol{x})} \tag{3.32a}$$

where

$$\boldsymbol{\chi} = (\kappa_1, \kappa_2 - \alpha\kappa_2, \kappa_3), \quad \boldsymbol{\kappa}_{13} = (\kappa_1, 0, \kappa_3); \quad A_{2n}(\boldsymbol{\chi}, t) = (k^2/|\boldsymbol{\chi}|^2) A_{2n}(\boldsymbol{\kappa}, t = 0) \tag{3.32b–d}$$

and

$$\partial^2\hat{\phi}_n/\partial x_2^2 - |\boldsymbol{\kappa}_{13}|^2\hat{\phi}_n = 0, \text{ subject to } \partial\hat{\phi}_n/\partial x_2 = A_{2n} \text{ on } x_2 = 0. \tag{3.32e}$$

From (3.21)–(3.23) Π_n, Q_{1n} and Q_{3n} can be calculated from Q_{2n}. When $\alpha = 0$ this is the solution for rapid changes in a turbulent flow when a rigid surface or 'wall' is introduced into the flow, and is valid over a period $0 < t \leqslant T_{\mathrm{L}}$ (see figure 3). Note that the solutions for u_1, u_2, u_3 (and their statistics) do not change over this timescale. The analysis can be generalized to allow for viscosity near the wall so that a no-slip boundary condition on the fluctuating velocity could be applied (Hunt & Graham 1978). The theoretical calculations for variances and spectra of different velocity components were compared with the laboratory experiments (that approximately correspond to the theoretical assumptions) of grid turbulence over a moving 'wall' by Uzkan & Reynolds (1967) (at low Reynolds number) and by Thomas & Hancock (1977) (at high Reynolds number). The different variations of the different components near the wall were well predicted, and good quantitative comparison was found for the normal components, even though the criterion (3.7*a*) for the RDT solution was not strictly satisfied. In fact, $T_{\mathscr{D}} \sim T_{\mathrm{L}}$ (Hunt 1984).

When $\alpha \neq 0$, all the velocity components (and the wavenumber component χ_2) in the shear flow change. A correlation $(-\overline{u_1 u_2})$ develops for the u_1 and u_2 components and energy is transferred to the streamwise component u_1. The ratio of $\overline{u_2^2}(x_2)$ near the

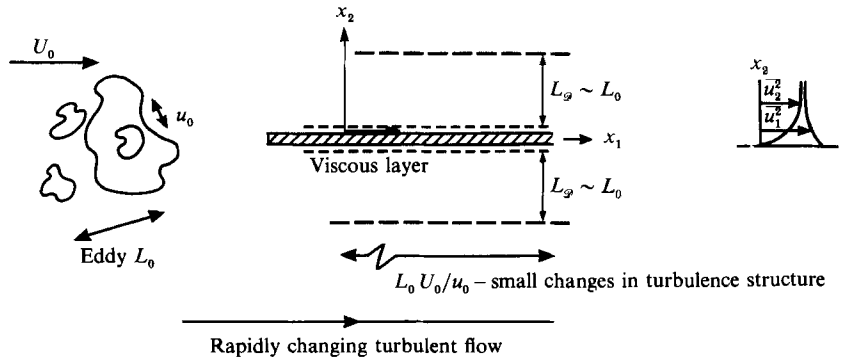

FIGURE 3. A rapidly changing turbulent flow for a rigid surface introduced into a flow. $L_{\mathscr{D}}$ and L_0 are the lengthscales of the inhomogeneous layer ($\mathscr{D}$), and of incident turbulence ($\mathscr{E}$).

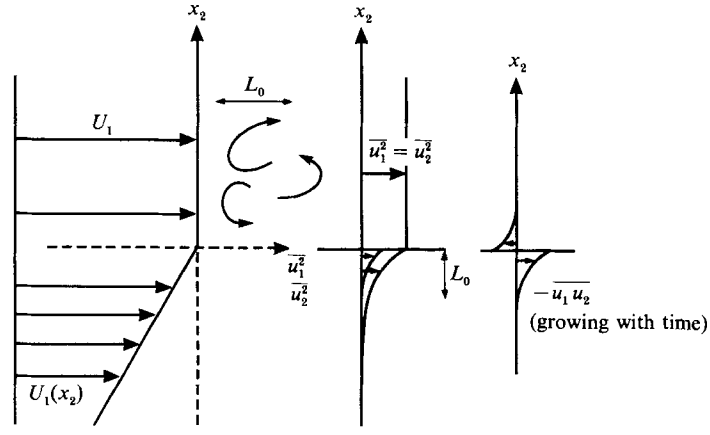

FIGURE 4. Interface between turbulence in a flow with uniform mean velocity and a shear flow that is initially non-turbulent.

wall compared with its value far from the wall is only slightly changed by shear (typically reduced by 20% for $\alpha t \approx 4$). In both cases at high Reynolds number, with or without a finite shear rate, it is found that $\overline{u_2^2} \propto \epsilon^{\frac{2}{3}} x_2^{\frac{2}{3}}$, if the high-wavenumber form of the energy spectrum $E(k)$ far from the boundary has the form $E(k) \propto \epsilon^{\frac{2}{3}} k^{-\frac{5}{3}}$.

Other solutions of inhomogeneous turbulence in shear flows have been obtained where the shear (α) changes at some plane, x_2 = constant. For example, consider a uniform velocity above a uniform shear (figure 4)

$$\boldsymbol{U} = (U_0, 0, 0) \quad \text{for} \quad 0 < x_2, \tag{3.33a}$$

$$\boldsymbol{U} = (U_0 + \alpha x_2, 0, 0) \quad \text{for} \quad x_2 < 0, \tag{3.33b}$$

and assume initially ($t \leqslant 0$) that the turbulence $\boldsymbol{u}_0(\boldsymbol{x}, t)$ is confined to the upper region $0 < x_2$. The solution for u_1 in terms of $\boldsymbol{u}_0(\boldsymbol{x}, t)$ obtained from (3.30), (3.31), and from additional constraints that u_2 and the pressure p are continuous across the surface at $x_2 = 0$, where the mean vorticity has a discontinuity (Gartshore *et al.* 1983).

At $t = 0$ the vorticity field in the upper region induces an irrotational fluctuating velocity field in the mean shear region ($x_2 < 0$) (Phillips 1955), and it decreases rapidly with $|x_2|$, i.e. $\overline{u_2^2} \propto (|x_2|/L_x)^{-4}$. As time increases, the mean shear leads to the shear stress $\overline{u_1 u_2}$ growing in this layer, and the amplification of the components u_1,

u_3, which can be computed from (3.32), (3.22). Note that the fluctuating pressure, which acts to reduce $-\overline{u_1 u_2}$ in the shear layer, also acts to produce a negative value of $-\overline{u_1 u_2}$ in the upper layer, because the pressure is continuous across $x_2 = 0$. (This important effect is not reproduced in current models of turbulent Reynolds stress or pressure strain rate, based on the local value of mean strain rate.) These idealized (but rational) methods have potential for further development to gain understanding of several important problems, such as complex interface regions at the edges of shear layers, when effects such as stratification, compressibility and rotation are important.

4. Some effects of shear and boundaries on the structure of turbulence

In this section we consider in detail the solutions of RDT for turbulence in uniform shear and near boundaries, and review the relevance of these solutions to understanding slowly changing turbulent shear flows.

4.1. *Specifying the uniform shear problem*

Consider a uniform shear flow $\boldsymbol{U} = (\alpha x_2, 0, 0)$ rapidly distorting, over a period $t_0 < t < t_1$, a homogeneous turbulent velocity field $\boldsymbol{u}$ whose initial energy spectrum at $t = t_0$ is $E_0(k)$. For homogeneous distorted turbulence, the velocity transfer functions are as defined in (3.16): $Q_{in}(\boldsymbol{\kappa}, \boldsymbol{x}, t) = A_{in}(\boldsymbol{\chi}, t)\,\mathrm{e}^{\mathrm{i}\boldsymbol{\chi}\cdot\boldsymbol{x}}$, where (from (3.16$c$)) the changing wavenumber is

$$\boldsymbol{\chi} = (\kappa_1, \kappa_2 - \beta\kappa_1, \kappa_3), \tag{4.1}$$

and $\beta = \alpha t$. Townsend (1970) derived the analytical solutions for the components of the amplitude function, A_{in}:

$$A_{11}(\boldsymbol{\chi}(k,t),t) = \left\{\frac{\beta\kappa_1^2}{k_{13}^2}\left(\frac{k^2 - 2\kappa_2^2 + \beta\kappa_1\kappa_2}{\chi^2}\right) - \frac{k^2}{k_{13}^3}\frac{\kappa_3^2}{\kappa_1}\left[\tan^{-1}\left(\frac{\kappa_2}{k_{13}}\right) - \tan^{-1}\left(\frac{\kappa_2 - \beta\kappa_1}{k_{13}}\right)\right]\right\} A_{22}(k, t_0), \tag{4.2a}$$

$$A_{22}(\boldsymbol{\chi}(k,t),t) = \frac{k^2}{\chi^2} A_{22}(k, t_0), \tag{4.2b}$$

$$A_{33}(\boldsymbol{\chi}(k,t),t) = \left\{\frac{\beta\kappa_1\kappa_3}{k_{13}^2}\left(\frac{k^2 - 2\kappa_2^2 + \beta\kappa_1\kappa_2}{\chi^2}\right) + \frac{k^2\kappa_3}{k_{13}^3}\left[\tan^{-1}\left(\frac{\kappa_2}{k_{13}}\right) - \tan^{-1}\left(\frac{\kappa_2 - \beta\kappa_1}{k_{13}}\right)\right]\right\} A_{22}(k, t_0), \tag{4.2c}$$

where k is the wavenumber at $t = 0$ and $k_{13}^2 = \kappa_1^2 + \kappa_3^2$.

Note that these expressions are independent of the magnitude of the wavenumber k, which is a special feature of homogeneous distortions!

The three-dimensional energy spectrum tensor $\boldsymbol{\Phi}_{ij}(\boldsymbol{\chi}, t)$ of the distorted turbulence is determined by its initial value $\boldsymbol{\Phi}_{0nm}(\boldsymbol{\kappa}, t = 0)$ and by $A_{in}(\boldsymbol{\chi}(\boldsymbol{\kappa}, t), t)$ from (3.17). The covariances $\overline{u_i u_j}$ are obtained by integrating $\boldsymbol{\Phi}_{ij}$ over all wavenumber space $\boldsymbol{\chi}$ or $\boldsymbol{\kappa}$. The initial spectrum $\boldsymbol{\Phi}_{0nm}(\boldsymbol{\kappa})$ is characterized by the isotropy of the variances of the components of turbulent velocity, i.e.

$$\int_{\boldsymbol{\kappa}} \boldsymbol{\Phi}_{0ij}\,\mathrm{d}\boldsymbol{\kappa} \Big/ \int_{\boldsymbol{\kappa}} \boldsymbol{\Phi}_{0ll}\,\mathrm{d}\boldsymbol{\kappa}$$

and of their distribution in wavenumber space, e.g.

$$\int_\kappa (\kappa_i \kappa_j/k^2) F_{0ll}\,\mathrm{d}\boldsymbol{\kappa} \Big/ \int_\kappa \Phi_{0ll}\,\mathrm{d}\boldsymbol{\kappa}$$

(cf. Kida & Hunt 1989), and by the distribution of turbulent energy over different scales, i.e.

$$E_0(k) = \frac{1}{2}\int_{|\boldsymbol{\kappa}|=k} \Phi_{0ll}(\boldsymbol{\kappa})\,\mathrm{d}A(\boldsymbol{\kappa}) \tag{4.3a}$$

(Batchelor 1953). In some cases the distribution of $\Phi_{0ij}(\boldsymbol{\kappa})$ over shells in wavenumber space is the same for all k, then

$$\Phi_{0ij}(\boldsymbol{\kappa}) = \hat{\Phi}_{0ij}(\hat{\boldsymbol{\kappa}})\, E_0(k), \tag{4.3b}$$

where $\hat{\boldsymbol{\kappa}} = \boldsymbol{\kappa}/k$ and $\displaystyle\int_{\hat{k}=1} \hat{\Phi}_{0ij}\,\mathrm{d}\hat{\boldsymbol{\kappa}} = 1.$

Since A_{in} is independent of k, the integral of (4.3) for the covariance $\overline{u_i u_j}$ can be written as

$$\overline{u_i u_i} = \int_0^\infty \left(\int_{|\boldsymbol{\kappa}|=k} A^*_{in} A_{jm}\, \Phi_{0nm}(\boldsymbol{\kappa})\,\mathrm{d}A(\boldsymbol{\kappa}) \right) \mathrm{d}k. \tag{4.4}$$

If $\Phi_{0ij}(\boldsymbol{\kappa})$ has the same form for all k, using expressions for A_{ij} normalized by k, (4.4) reduces to

$$\overline{u_i u_j}(t) = \overline{u_{0l} u_{0l}} \int_{|\boldsymbol{\kappa}|=k} A^*_{in}(\hat{\boldsymbol{\kappa}})\, A_{jm}(\hat{\boldsymbol{\kappa}})\, \hat{\Phi}_{0nm}(\hat{\boldsymbol{\kappa}})\,\mathrm{d}\hat{\boldsymbol{\kappa}}. \tag{4.5}$$

4.2. *Covariances*

Results for $\overline{u_i u_j}$ have been obtained for two cases where the turbulence is initially isotropic or initially axisymmetric about the streamwise direction x_1, and Φ_{0ij} is given by (3.14*a*) or (3.15) (Maxey 1982).

For a small time after the shear has been applied ($\beta < 1$), A_{in} can be expanded in powers of β and the integral (4.5) can be calculated analytically, leading to

$$\overline{u_1^2}(t) = \overline{u_1^2}(0) + \left(\underline{1} - \frac{25+9(R-1)}{35}\right)\beta^2 \overline{u_2^2}(0), \tag{4.6a}$$

$$\overline{u_2^2}(t) = \overline{u_2^2}(0) - \left(\frac{4+2(R-1)}{35}\right)\beta^2 \overline{u_2^2}(0), \tag{4.6b}$$

$$\overline{u_1 u_2}(t) = -\overline{u_2^2}(0)\left(\underline{1} - \frac{3+(R-1)}{5}\right)\beta(1+O(\beta^4)), \tag{4.6c}$$

$$\overline{u_3^2}(t) = -\overline{u_3^2}(0) + \left(\frac{4(R-1)}{35}\right)\beta^2 \overline{u_2^2}(0), \tag{4.6d}$$

where $R = \overline{u_1^2}/\overline{u_2^2}(t=0) = \overline{u_1^2}/\overline{u_3^2}(t=0)$. The terms underlined show how $\overline{u_1^2}$ and $-\overline{u_1 u_2}$ increase solely because of horizontal momentum changes caused by vertical motion of fluid elements (i.e. by the term $u_2 \partial U_1/\partial x_2$ in the momentum equations) or by bending and stretching of the mean vorticity (i.e. the term $\Omega_3 \partial u_2/\partial x_3$, $\Omega_3 \partial u_3/\partial x_3 \approx \Omega_3 \partial u_2/\partial x_2$ in the vorticity equations). These terms dominate if eddies are elongated in the streamline direction (Landahl 1984). Note how these changes just depend on the vertical turbulence $\overline{u_2^2}$. The other terms contributing to the change in $\overline{u_i u_j}$ can be also considered as corrections associated with the spheroidal shape

of eddies (Landahl 1984; Auton, Hunt & Prud'homme 1988) (i.e. the pressure gradient terms in the momentum equation) or the rotation and stretching by the mean flow of the fluctuating velocity (i.e. $(\boldsymbol{\omega}\cdot\boldsymbol{\nabla})\,\boldsymbol{U}$ in the vorticity equation). These corrections depend on the anisotropy of the variances of the components of the initial turbulence and their distribution wavenumber space. So it is not surprising that approximate models of turbulence differ from each other and from the above results (which are only strictly valid for small times).

When the strain is finite ($\beta \gtrsim 1$), evaluating the integral (4.5) requires computation. It is found that the way that $\overline{u_i u_j}$ changes with small strain continues with larger strain, i.e. $\overline{u_1^2}$ and $\overline{u_3^2}$ increase without limit, $-\overline{u_1 u_2}$ increases to a limiting value, and $\overline{u_2^2}$ continues to decrease. For large strain when $\beta \gg 1$, $\overline{u_1^2} \propto \beta$, $\overline{u_2^2} \propto \ln\beta$ and $\overline{u_2^2} \propto (\ln\beta)/\beta$ (Rogers 1990). The Reynolds shear stress is simply related to $\overline{u_1^2}$ from the kinetic energy equation. Since $\overline{u_i u_i} \to \overline{u_1^2}$, $-\overline{u_1 u_2} \to \overline{u_1^2}/2\beta \to$ constant as $\beta \to \infty$. The initial state of the turbulence does not effectively change the relative orders of magnitude of the moments but it does change their actual values. For isotropic turbulence $\rho_{12} \approx 0.6$, when $\beta \approx 2$, but for anisotropic axisymmetric turbulence, ρ_{12} is reduced. For $R = 2$, $\rho_{12} = 0.4$ (Maxey 1982).

Suitable parameters for defining the distortion of different flows are the second invariants $\mathrm{II}_u = -\frac{1}{2}b_{ij}\,b_{ji}$ and $\mathrm{II}_\omega = -\frac{1}{2}W_{ij}\,W_{ji}$ of the anisotropy tensor of the moments of velocity $b_{ij} = \overline{u_i u_j}/\overline{u_l u_l} - \frac{1}{3}\delta_{ij}$, and of vorticity $W_{ij} = \overline{\omega_i \omega_j}/\overline{\omega_l \omega_l} - \frac{1}{3}\delta_{ij}$ (Lumley 1978). As the shear strain β increases to 2, for initially anisotropic turbulence, $-\mathrm{II}_u$ increases from 0 to 0.05; whereas for initially axisymmetric turbulence $-\mathrm{II}_u$ increases less, from 0.02 to 0.03. Even when $\beta = 10$, $-\mathrm{II}_u = 0.2$ and $-\mathrm{II}_\omega = 0.05$, which are about two-thirds of their limiting values of 0.33 and 0.083 (Lee *et al.* 1988). The explanation is that, when $\beta \gg 1$, $u_1^2 \gg u_2^2, u_3^2$ and $\omega_2^2, \omega_3^2 \gg \omega_1^2$.

4.3. *Comparison with nonlinear computations and experiments*

The RDT results can be compared with exact direct numerical simulations (DNS) of the viscous nonlinear Navier–Stokes equations, and, unlike comparisons with experiments, these can be defined rather precisely with exactly the same initial conditions.

We recall the argument of §3 that the linear RDT theory should give a good approximation to the most amplified components of turbulence over an arbitrary straining time (i.e. $T_{\mathscr{D}} > T_{\mathrm{L}}$), if the linear strain rate is large compared with the nonlinear strain rate (i.e. $\mathscr{S}^* = (\mathrm{d}U_1/\mathrm{d}x_2)\,L_x/u_0 \gg 1$). But the components of turbulence that are diminished (in physical or wavenumber space) are likely to be poorly modelled by RDT.

Lee *et al.* (1988) compared the inviscid RDT solutions of isotropic turbulence in homogeneous shear with the results of DNS where the initial state of turbulence was fully developed homogeneous turbulence with a Reynolds number Re_d of about 40. The results for the anisotropy defined by the second invariant II (figure 5) show that in this case, the linear solution closely approximates to the exact result. This is to be expected since $\mathscr{S}^*$ is much greater than unity; in fact $\mathscr{S}^* \approx 10$.

Note that the linear solution slightly underestimates the anisotropy. This contradicts the usual assumption that the nonlinear straining (ignored in linear theory) always reduces anisotropy (see §3.1).

We have seen that for turbulence in homogeneous shear, the Reynolds stress coefficient $\rho_{12} = -\overline{u_1 u_2}/(\overline{u_1^2}\,\overline{u_2^2})^{\frac{1}{2}}$ for homogeneous shear decreases quite markedly if the initial anisotropy ($R = \overline{u_1^2}/\overline{u_2^2}$) increases. This is an alternative explanation for why the value of ρ_{12} is greater than the experimental value, when the initial

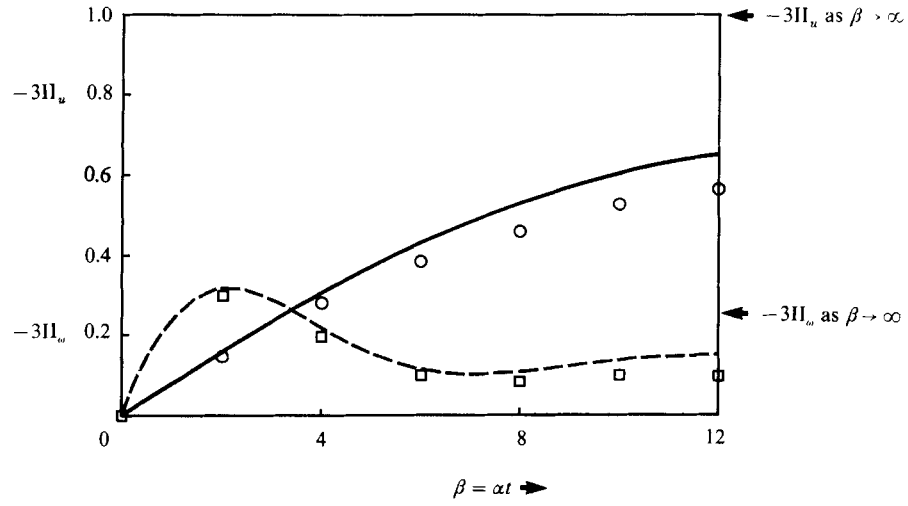

FIGURE 5. Comparison of anisotropy in homogeneous turbulent shear flow of the velocity variances (where $\overline{u_1^2} > \overline{u_2^2} \gg \overline{u_3^2}$) and the vorticity variances (where $\overline{\omega_2^2}, \overline{\omega_3^2} \gg \overline{\omega_1^2}$), as calculated by DNS and RDT. The anisotropy is defined by the second invariants II_u, II_w. DNS: ○, $-II_u$; □, $-II_w$. RDT: ——, II_u; – – –, II_ω. (From Lee *et al.* 1988.)

turbulence is isotropic, which differs from that of Jeandel *et al.* (1978) and Townsend (1976), who assumed that the small-scale dissipation of turbulent energy reduced ρ_{12}, because this dissipation has a stronger effect on $-\overline{u_1 u_2}$ than on $\overline{u_1^2}$. At this stage it is not clear which mechanism is most significant.

4.4. *Spectra*

To investigate how the spatial structure of the turbulence changes with shear, 'two-point' spectra can be calculated using (4.2) and (4.3). We are particularly interested in the form of the spectra at high wavenumber to see whether there are any universal features of the small-scale turbulence in shear flow.

It is instructive to express the spectra in terms of the local wavenumber χ. In a shear flow after a finite distortion the spherical surface of $\chi = \text{constant}$ in wavenumber space corresponds to a surface

$$\chi^2 = \kappa_1^2 + (\kappa_2 - \kappa_1 \beta)^2 + \kappa_3^2, \tag{4.7}$$

which in $\boldsymbol{\kappa}$-space is a spheroid flattened in the κ_2 direction, rotated and elongated in the direction $\kappa_2 = \kappa_1 \beta$.

After some algebra, the components $E_{ii}(\chi)$ of the energy spectrum $E(\chi)$ are found to have the forms

$$E_{11}(\chi) = \int_{\chi=\text{const}} \frac{E_0(k)}{4\pi k^2} \left\{ \frac{k^2}{k_{13}^2}(a+b)\left((a+b) - \frac{2\kappa_1\kappa_2}{k^2}\right) + \frac{k_{23}^2}{k^2} \right\} \mathrm{d}A(\boldsymbol{k}), \tag{4.8a}$$

$$E_{22}(\chi) = \int_{\chi=\text{const}} \frac{E_0(k)}{4\pi} \frac{k_{13}^2}{\chi^4} \mathrm{d}A(\boldsymbol{\kappa}), \tag{4.8b}$$

$$E_{33}(\chi) = \int_{\chi=\text{const}} \frac{E_0(k)}{4\pi k^2} \left\{ \frac{\kappa_1^2 \kappa_3^2}{k^2 k_{13}^2} \left(\frac{-k^2}{\kappa_3^2} a + \frac{k^2}{\kappa_1^2} b \right)^2 - \frac{2\kappa_1 \kappa_3^2 \kappa_2}{k^2 k_{12}^2} \left(\frac{-k^2}{\kappa_3^2} a + \frac{k^2}{\kappa_1^2} b \right) + \frac{k_{23}^2}{k^2} \right\} \mathrm{d}A(\boldsymbol{\kappa}), \tag{4.8c}$$

where $$a = \frac{-\kappa_3^2}{\kappa_1 k_{12}}\left[\tan^{-1}\left(\frac{\kappa_2}{k_{13}}\right) - \tan^{-1}\left(\frac{\kappa_2 - \beta\kappa_1}{k_{13}}\right)\right]$$

and $$b = \beta\kappa_1^2(k^2 - 2\kappa_2^3 + \beta\kappa_1\kappa_3)/k^2\chi^2.$$

Also $k^2 = \chi_1^2 + (\chi_2 + \beta\chi_1)^2 + \chi_3^2 = \chi^2[\cos^2\theta + (\sin\theta\cos\phi + \beta\cos\theta)^2 + \sin^2\theta\sin^2\phi]$

and $$\mathrm{d}A(\boldsymbol{k}) = k^2\sin\theta\,\mathrm{d}\theta\,\mathrm{d}\phi,$$

where $\chi = |\boldsymbol{\chi}|$. The form of $E_0(k)$ has to be broadly specified in order to obtain asymptotic results for $E(\chi)$ when $\chi \gg L^{-1}$ and $\beta \gg 1$. Over the sphere in $\boldsymbol{\chi}$ wavenumber space on which χ is constant and large, defined by (4.7), $|\boldsymbol{\kappa}|$ is very small and $\kappa_1 \sim \chi/\beta$, $\kappa_2 \sim \chi$ and $\kappa_3 \leqslant \chi$. Since $E_0(k)$ decreases with k when $kL_x \gg 1$, it follows that when $\beta \gg 1$, the integral is determined by the distribution of the large-scale energy of the initial turbulence.

If the initial turbulence consists of isolated volumes of flow such as vortex rings with dimension L_2, which are separated by a distance of L_1, then

$$E_0(k) \propto k^2 \quad \text{when} \quad L_1^{-1} \ll k \ll L_2^{-1}. \tag{4.9}$$

But if the initial turbulence consists of vortex tubes with diameter of order L_3 and lengths of order L_2 (e.g. the vortex ring diameter)

$$E_0(k) \propto k^0 \quad \text{when} \quad L_2^{-1} \ll k \ll L_3^{-1} \tag{4.10a}$$

$$E_0(k) \propto k^2 \quad \text{when} \quad k \ll L_1^{-1}. \tag{4.10b}$$

Inspection and kinematical analysis of the turbulent flows computed using DNS (at $Re_\lambda \leqslant 100$) indicate that the 'tangled-vortex tube' model is a good description of the flow structure, for a broad class of sheared and unsheared flows (e.g. Wray & Hunt 1989; Adrian & Moin 1989). For sufficiently large scales ($k \ll L_1^{-1}$) there is some evidence from computation (Lesieur 1987) that $E_0(k) \propto k^4$ (as derived by Batchelor & Proudman 1956). But Saffman (1967) gave a counter example of turbulence where $E_0(k) \propto k^2$, as $k \to 0$.

The spectra for the small scales of turbulent flows appear to be highly dependent on the Reynolds number (e.g. Re_λ) of the turbulence and on the mean velocity distribution. For fully developed turbulence generated by grids in wind tunnels, or obtained by DNS, without mean shear (where $Re_\lambda \leqslant 300$) the spectra decrease rapidly with k, typically $E(k) \propto \mathrm{e}^{-k^2L^2}$ at the lowest values of Re_λ (Champagne, Harris & Corrsin 1970; Rogallo 1981), and $E(k) \propto k^{-n_H}$, where $n_H \gtrsim 2$, at the higher values of Re_λ). However, in shear flows, even at these ranges of Re_λ, it is quite usual to find that $E_0(k)$ decays algebraically, i.e. $E_0(k) \propto k^{-n}$ when $-\frac{5}{3} \leqslant n \leqslant 2$ – over a significant range. In typical wind-tunnel boundary layers, the small-scale spectrum changes from exponential decay in the outer region to algebraic decay (k^{-2}) near the surface (Bradshaw 1967). For example, Ho & Huerre (1984) find that in a mixing layer n lies in this range just after about three 'pairings' of the large vortices in the shear layer, beyond which point the turbulence has a complex three-dimensional structure. Rogallo (1981) found $n \to 2$ in his computations of turbulence in a homogeneous shear flow which extended to $\beta = 18$ but Rogers & Moin (1987) found that $n \approx 3$ for $\beta = 8$. In Champagne *et al.*'s (1970) wind-tunnel measurements they found that $n = 2$, even for quite small strain (see figure 6). Wherever the Reynolds number is high enough, such as in atmospheric or oceanic turbulent flows ($Re_\lambda \gtrsim 10^4$), the small-scale structure of shear flows is described by the Kolmogorov inertial range theory, with $n = \frac{5}{3}$.

Although in these model computations we focus on the spectra where $\chi L_x \gg 1$, we have to define the initial spectra over a wide range of wavenumber. We consider the two forms

$$E_0(k) = u_0^2 L(kL)^N \exp(-k^2L^2) \quad \text{where } N \text{ is integer and } N \geqslant 0, \tag{4.11a}$$

and

$$E_0(k) = \frac{u_0^2 L}{(1+(kL)^2)^P}, \quad \text{where } 1 < P. \tag{4.11b}$$

The form of $E(\chi)$ when $\beta \gg 1$ can be derived by asymptotic analysis of the integrals in (4.8). In the range $1 \ll \chi L \ll \beta$ an examination of the terms shows that these are dominated by E_{11}, so that $E_{11}(\chi) \approx E(\chi)$ and

$$E(\chi) \propto \frac{\int_{\chi=\text{const}} \beta^2 E_0(k(\chi)L)\,\mathrm{d}A(\boldsymbol{\kappa})}{k^2}. \tag{4.12}$$

The integrals are dominated by a narrow region in wavenumber space, defined by $|\hat{\theta}| \ll 1$ and $|\phi| \ll 1$, where $\hat{\theta} = \frac{1}{2}\pi + (1/\beta) - (\theta/\beta)$. Therefore, when $\beta \gg 1$,

$$E(\chi) \propto \int_{-\infty}^{\infty}\int_{-\infty}^{\infty} \frac{\beta E_0([\chi^2L^2/\beta^2 + \chi^2L^2(\hat{\theta}^2+\phi^2)]^{\frac{1}{2}})}{\chi^2L^2}\,\mathrm{d}(\hat{\theta}\chi L)\,\mathrm{d}(\phi\chi L).$$

Thus for the range $1 \ll \chi L \ll \beta$, if $E_0(k) = o(k^{-2})$ when $kL \gg 1$,

$$E(\chi) \propto \beta\left(\int_0^{\infty} \hat{k}E_0(\hat{k})\,\mathrm{d}\hat{k}\right)/\chi^2L^2. \tag{4.13}$$

So whatever the initial spectrum, provided it decreases faster than k^{-2}, for large enough strain, over an increasing range of wavenumber, the energy spectrum tends to the limiting form of

$$E(\chi) \propto \beta\chi^{-2}. \tag{4.14}$$

This result holds for broader classes of spectra than those specified in (4.11).

However if the initial spectrum decreases slower than k^{-2} as k increases, the integral $\int_0^{\infty} \hat{k}E(\hat{k})\,\mathrm{d}\hat{k}$ does not converge, even though the integrand is still dominated by the narrow region of wavenumber space where

$$\kappa_1 \ll L^{-1}/\beta, \quad \kappa_2 \sim \beta L^{-1}, \quad \kappa_3 \sim L^{-1}.$$

Thus for turbulence at very high Reynolds number, where there is a $-\frac{5}{3}$ spectrum, the effect of shear is to maintain a $-\frac{5}{3}$ spectrum, which has been well established in many field experiments (e.g. see Monin & Yaglom 1971; Wyngaard & Cote 1972).

Computations of $E_{ii}(\chi)$ for the streamwise and vertical velocity components are displayed in figure 7 (for the simple spectrum $E(k) \propto \exp(-k^2L^2)$). These show a tendency to the χ^{-2} spectrum, for the streamwise component and χ^{-4} for the vertical component (χ^2) when the initial spectrum decays faster than k^{-2}.

It is also instructive to compute the one-dimensional spectra $\Theta_{ij}(\chi_l)$ in different directions to show the anisotropy of the turbulent structure. Also, these are the spectra that are usually measured. Figure 8(*a–c*) shows that the one-dimensional spectra of $\Theta_{11}(\chi_2)$ in the direction χ_2 vertically across the flow demonstrate χ_2^{-2} spectra; but for wavenumbers parallel to the flow the $\Theta_{11}(\chi_1)$ spectrum is proportional to $\mathrm{e}^{-(\chi_1 L)^2}$, if $E_0(k) \propto \mathrm{e}^{-k^2L^2}$. But if the axes for defining spectra (indicated by a prime) are rotated slightly at an angle θ' from the flow direction, so that χ_1 becomes χ_1', then $\Theta_{11}'(\chi_1') \propto \chi_1'^{-2}$. (The same forms are found for different initial spectra as defined in (4.11).) (These variations in $\Theta_{11}(\chi_l)$ for different χ_l are smeared out by the effects of

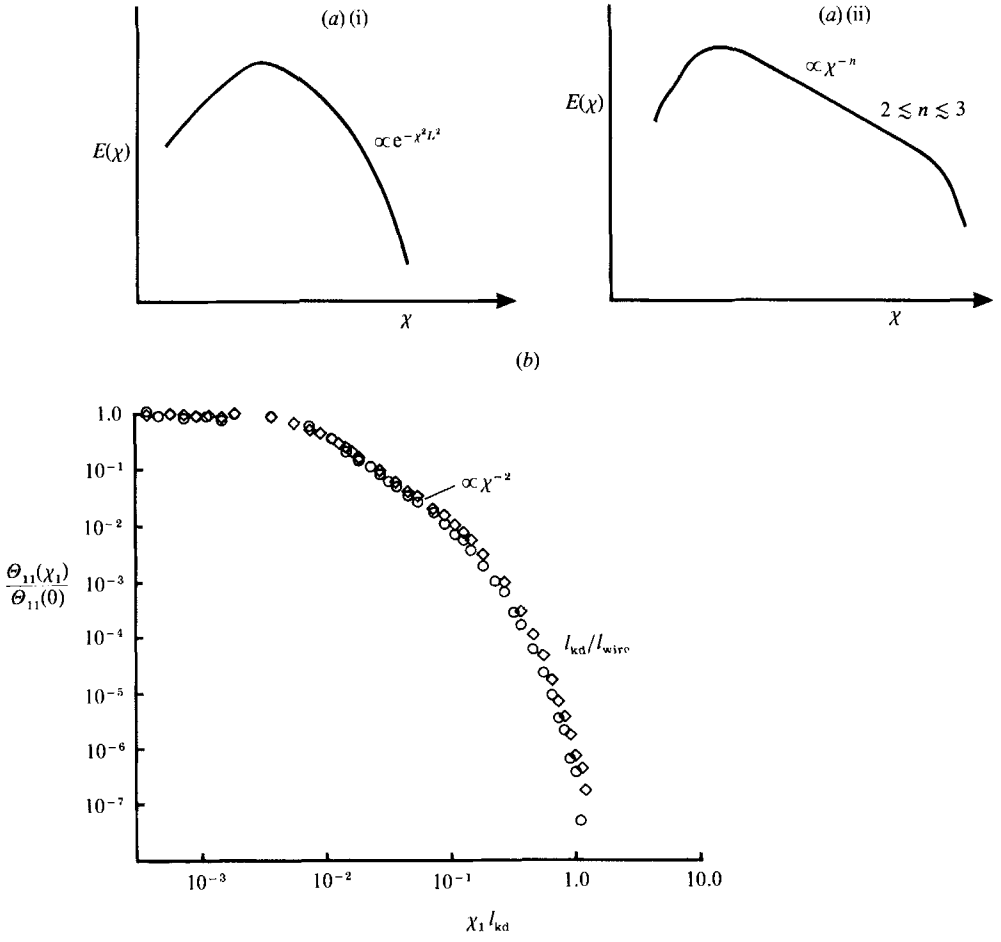

FIGURE 6(*a*, *b*). For caption see facing page.

large-scale turbulence randomly rotating the vorticity of small-scale eddies when $T_{\mathscr{D}} \geqslant T_{\mathrm{L}}$ (Kida & Hunt 1989).)

There is a simple physical explanation of these spectra which are only found where vortex sheets exist (on a scale much less than χ^{-1}). In this case, the 'vortex sheets' are high localized gradients $\partial u_1/\partial x_2, \partial u_1/\partial x_3$, which surround long, narrow regions or 'streaks', where the streamwise fluctuations are positive or negative. These phenomena have been seen in direct numerical simulation of individual flow realizations, and in experiments (Lee *et al.* 1988). Similar structures were observed by representing a set of realizations of the flow field as

$$u_i(\boldsymbol{x}, t) = \sum_{n\text{-space}} A_{in}(\boldsymbol{x}, t)\, \mathrm{e}^{\mathrm{i}(\boldsymbol{x}\cdot\boldsymbol{\kappa}_n)} S_{0n}(\boldsymbol{\kappa}_n),$$

where S_{0n} is randomly distributed (subject to its variance being proportional to the spectrum) and where the deterministic velocity transfer function A_{in} is given by RDT (figure 9) (Carruthers, Fung & Hunt 1989).

The essential result of the linear theory is to show that the form of the high-wavenumber spectra in most turbulent shear flows is largely determined by the linear distortion effects of the mean shear rather than by nonlinear interactions, and that

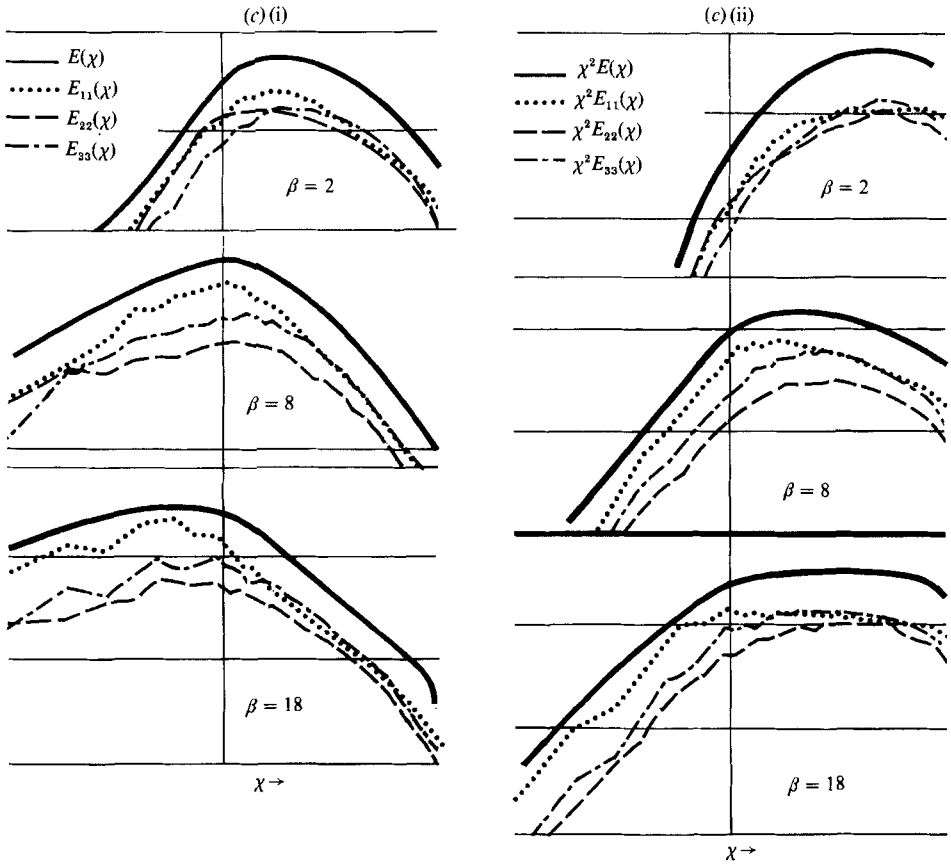

FIGURE 6. Changes in the energy spectra caused by shear. (*a*) Schematic diagram (i) before shear, (ii) after shear. (*b*) One-dimensional spectrum measured by Champagne *et al.* (1970) in shear flow at two positions downstream. ○, $x_1/h = 10.5$; ◇, $x_1/h = 8.50$; h is the height of the wind tunnel, l_{kd} is the Kolmogorov microscale. (*c*) Direct numerical simulations of Rogallo (1981) of homogeneous turbulence in uniform shear ($Re_\lambda \approx 80$). (i) $E(\chi)$, $E_{ii}(\chi)$; (ii) $\chi^2 E(\chi)$, $\chi^2 E_{ii}(\chi)$.

the algebraic form of these spectra is consistent with the existence of discontinuities in velocity or velocity gradients on the scale of L/β.

5. Discussion and tentative conclusions

In this review we have described some developments in the techniques of RDT and in the general understanding of how it can be used; in particular that the theory provides a rational basis for analysing 'rapidly changing turbulent flows' (RCT), and a heuristic method for estimating certain features of 'slowly changing turbulent flows' (SCT).

5.1. *RDT 'Statistical eigensolutions'*

There are certain features of turbulent flow structure predicted in which moments of certain components of the turbulent velocity reach a steady state, or change very slowly, even when the turbulence is being rapidly distorted. These are 'eigensolutions', in the sense that, if the initial turbulence was specified to have these forms, the particular statistical features of the turbulence would change little under the action of the distortion (provided it was rapid). In the first case, of inhomogeneous

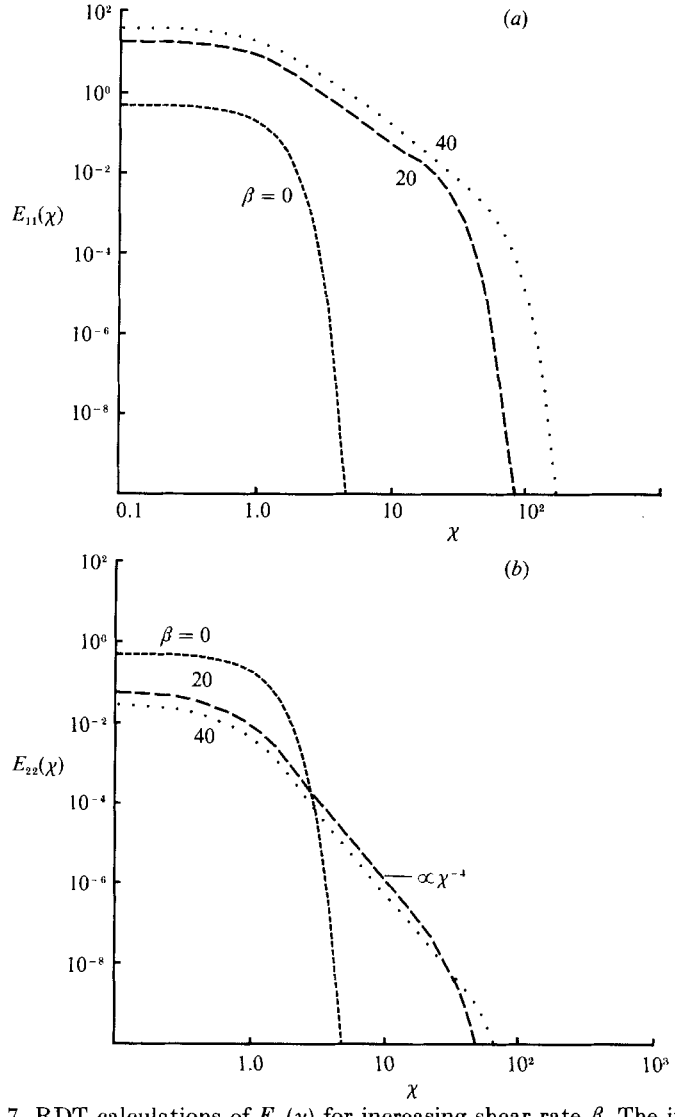

FIGURE 7. RDT calculations of $E_{ii}(\chi)$ for increasing shear rate β. The initial spectrum is $E_0(k) = u_0^2 L\, e^{-(k^2L^2)}$. (*a*) $E_{11}(\chi)$; (*b*) $E_{22}(\chi)$.

turbulence near a rigid surface, $x_2 = 0$, with or without mean shear, these features are moments such as $\overline{u_2(x_2')\, u_2(x_2)}/\overline{u_2^2(x_2)}$, $\overline{u_2(x_2')\, u_2(x_2)}/(\overline{u_1^2}\,\overline{u_2^2})^{\frac{1}{2}}$, and other components. These correlations depend weakly on the initial anisotropy and the form of the energy spectra.

In the second case, of locally homogeneous turbulence in a uniform shear, these features include the shear-stress cross-correlation coefficient

$$\rho_{12} = -\overline{u_1(x_1)\, u_2(x_2)}/(\overline{u_1^2}\,\overline{u_2^2})^{\frac{1}{2}},$$

which changes very slowly ($\propto \ln^{-\frac{1}{2}}\beta$, for $\beta \gg 1$) and the structure function, which, for a wide class of flows, becomes proportional to the spacing, $|\boldsymbol{r}|$, when it is much less than the largest scales and much greater than the scales controlled by viscosity, i.e.

$$\overline{(u_i(\boldsymbol{x}) - u_i(\boldsymbol{x}+\boldsymbol{r}))^2} = B|\boldsymbol{r}|. \tag{5.1}$$

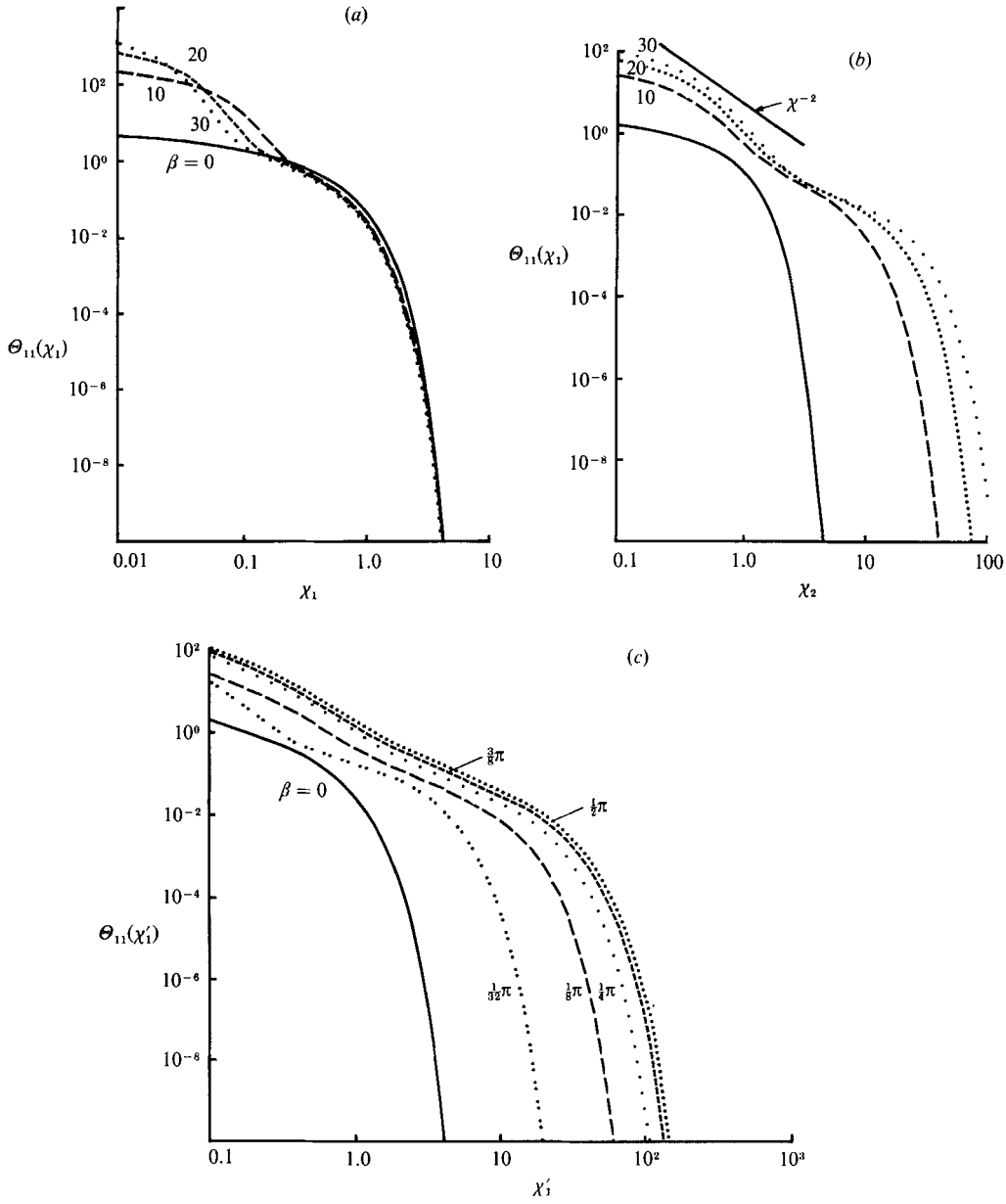

FIGURE 8. $\Theta_{ii}(\chi_j)$ calculated by RDT in uniformly sheared flow. The initial spectrum is $E_0(k) = u_0 L\, e^{-(k^2L^2)}$. (*a*) $\Theta_{11}(\chi_1)$; (*b*) $\Theta_{11}(\chi_2)$; (*c*) $\Theta'_{11}(\chi'_1)$. The axes for defining the spectrum are rotated by an angle θ' (in ther χ_1, χ_2-plane) from the flow direction.

(This is equivalent to the energy spectra $E(\chi)$ becoming proportional to χ^{-2} over a range of χ, when $\beta \gg 1$.) The proportionality factor $B(\sim \beta u_0^2 L_0$ with dimensions $LT^{-2})$ increases with time, with the shear $\mathrm{d}U_1/\mathrm{d}x_2$, and with the initial kinetic energy of the turbulence u_0^2, but inversely with the initial lengthscale L_0 (defined by $\int_0^\infty k^{-1}E(k)\,\mathrm{d}k/u_0^2$). In this case the shear-stress cross-correlation coefficient depends on the anisotropy of the initial spectrum, but not the form of the spectrum, whereas the form of the structure function and the energy spectra (over a given range of $|r|$ and

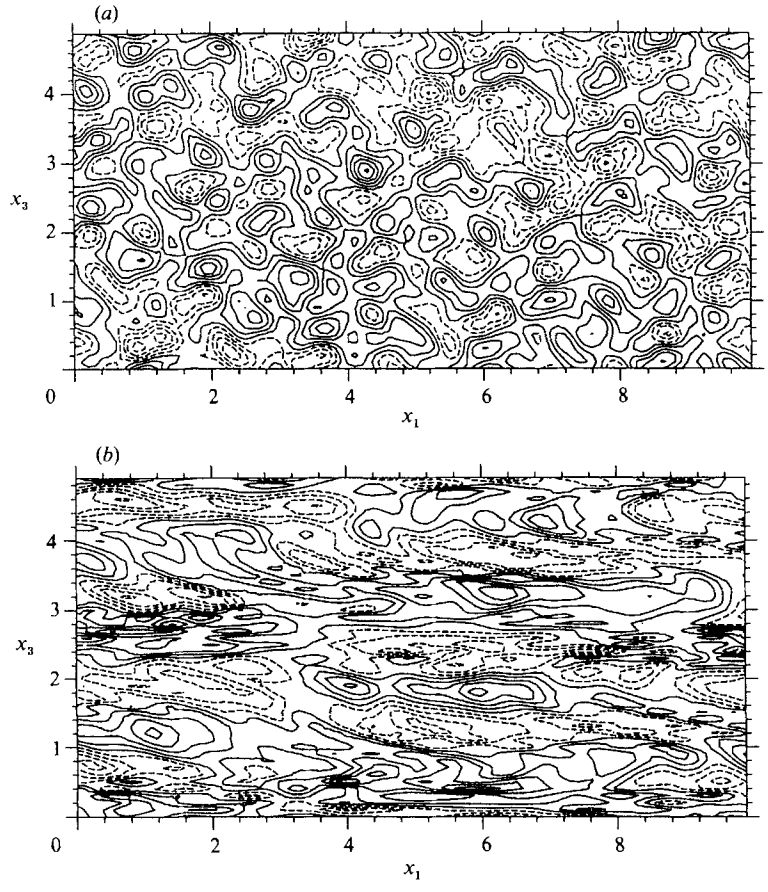

FIGURE 9. Realizations of homogeneous turbulence as shown by contour lines of u_1 in the (x_1, x_3)-plane. (*a*) Isotropic turbulence, $E_0 = L^3 u_0^2 k^2 e^{-k^2 L^2}$. (*b*) After a rapid distortion. $\beta = \alpha t = 11.7$. ($\mathscr{S}^* = \alpha L/u_0 = 40$.) Note the sharp gradients in the x_3 direction (consistent with $E \propto \chi^{-2}$) and the elongated contours in the x_1 direction (consistent with figure 8*a*, *c*).

χ) tends to become independent of the initial turbulence, provided that in the initial spectra $E_0(k) = o(k^{-2})$ when $k \gg L^{-1}$.

5.2. *Extrapolation of results to slowly changing turbulence*

The nonlinear processes in a turbulent flow can only be estimated and modelled approximately; but it is clear that they affect the energy and anisotropy of the turbulence on a timescale L/u_0. So, if the turbulence is distorted significantly on this timescale by a linear process (i.e. $\mathscr{S}^* \gg 1$), the effect of the nonlinear terms is approximately equivalent to a continual change in the initial conditions of RDT calculations. Therefore if certain results of the RDT calculation (the 'statistical eigensolutions') are not only changing slowly with time, but are approximately independent of the anisotropy and energy spectrum of the initial turbulence, the form of these RDT solutions also approximately describes turbulent flows that persist over many timescales, i.e. slowly changing turbulent flows, such as shear flows and flows bounded by a rigid surface (Hunt 1984) or density interface (Carruthers & Hunt 1986). The numerical values of the coefficients, such as ρ_{12}, of these 'eigensolutions', depend on the initial anisotropy, and consequently different

coefficients can be expected in different turbulent flows with different initial and boundary conditions.

This is essentially the argument for using the results of RDT to provide new insights and practical models for many kinds of SCT.

More complete models of SCT require modelling and understanding the effects of the nonlinear processes, one aspect of which is the random mean distortion of small-scale turbulence by large scales, and the transfer of energy between the scales. Over short periods, this is a problem of RDT with a random distortion tensor α_{ij}. Using this method, Kida & Hunt (1989) found that the qualitative effects of interaction between the scales in the presence of mean strain are not, in general, the same as in the absence of mean strain; for example the tendency of these interactions to make the turbulence more isotropic may be weaker. Consequently, in slowly changing turbulent flows, the nonlinear processes cannot be assumed to have a strong tendency of returning the turbulence to isotropy. This is another reason why it is not necessarily valid to assume that the appropriate initial condition for RDT computations for SCT is that the turbulence is isotropic.

5.3. *The structure of shear flows: some new insights from RDT*

Another way of understanding the generation of the different components of turbulent shear stresses and pressure gradients is to study the dynamics in individual eddies. The form of these energy-containing eddies can be derived from the two-point cross-correlations (Townsend 1970, 1976), or from inspection of the different computed realizations of the flow field (e.g. Lee *et al.* 1988). (These may not be the largest eddies spanning the whole flow.) The structure predicted by RDT (given the appropriate value of the mean strain, β) agrees well with the measurements.

This predicted structure, with its significant streamwise and antistreamwise vorticity ('double-roller eddies'), and localized regions of intensified transverse vorticity and intense streamwise velocity (or streaks), is therefore different to the structure of the linear eigenmodes of the mean velocity profile predicted by hydrodynamic stability theory. The corollary is that if the results of RDT are to be used for estimating Reynolds stress or pressure gradients etc., then they are only valid where the eddy structure has a similar form to that predicted by RDT. Therefore the use in fully developed turbulent shear flows of turbulence models (such as that of Launder, Reece & Rodi 1975 or Lumley 1978) in which the forms of the cross-correlations of velocity and pressure gradient are the same as those predicted by RDT implies that the structure of the energy-containing eddies is similar to that of three-dimensional turbulence in homogeneous shear. Experimental studies of free-shear layers have shown that this kind of eddy structure occurs in the 'later' or 'far downstream' stage of free-shear layers, while in the 'early' stages the eddy structure is similar to the eigenmodes. (This transition is very clear in computations and measurements of wakes; Lesieur & Métais 1989; Mumford 1982.) This suggests that knowing the eddy structure of turbulence, perhaps by flow visualization, indicates where models based on three-dimensional turbulence in local straining flows (such as RDT or 'closure models') are likely to be valid. (So one would not expect such local turbulence models to describe satisfactorily the turbulence in the near wakes of bluff obstacles in cross-streams; Murakami & Mochida 1988.)

The asymptotic result from RDT about the form of the energy spectrum of turbulence in uniform shear flow, given by (4.14), has a number of general implications about the interpretation of computations and measurements and about the generality of models of turbulent shear flows.

If the Reynolds number of turbulence is too low for the smallest scales to be independent of the largest scales (which in practice means that $Re_\lambda \lesssim 10^3$), then the energy spectrum cannot have an inertial subrange. In the presence of shear, RDT theory and the hypothesis of §4.4 suggests that, even for slowly changing turbulent flows, the small-scale spectrum tends to a form where $E(k) \propto k^{-2}$, whatever the initial form of the spectrum of turbulence. The 'initial' form may result from nonlinear three-dimensional instabilities in free-shear flows or Orr–Sommerfeld instabilities in wall layers, but the important point is that, under the action of linear processes, the small-scale turbulence tends to a general form.

It has already been remarked in §4.4 that there have been many experiments at low-to-moderate Reynolds number $Re_\lambda \leqslant 200$, where spectra (either energy or one-dimensional) approximate to this form.

The major implications of the spectra of low-Reynolds-number turbulence changing to this form are that

(i) the strain rates of the small scales become comparable with large scales, so that energy production at small scales becomes significant (e.g. vortex streets becoming unstable or small-scale production associated with longitudinal vortices). Presumably, therefore, the presence of shear can stimulate the nonlinear cascade of energy. Indeed, one form might be a repetition of the vortex sheet and 'streak' structure within the vortex sheets formed by the linear distortion;

(ii) from (5.1), the mean shear determines the magnitude of the smallest scales of motion, which are controlled by viscous stresses and defined by velocity and length scales u_ν, l_ν. Since $u_\nu l_\nu/\nu \sim 1$, it follows that

$$l_\nu \sim \nu^{\frac{3}{4}}/B^{\frac{1}{2}}, \quad L/l_\nu \sim (Lu_0/\nu)^{\frac{3}{4}}\beta^{\frac{1}{2}}. \tag{5.2}$$

Therefore the ratio of the largest-to-smallest scales increases as the strain ratio increases, but does not increase quite as rapidly with (lu_0/ν) as in very high-Reynolds-number turbulence, where

$$(L/l_\nu) \sim (Lu_0/\nu)^{\frac{3}{4}}; \tag{5.3}$$

(iii) the dissipation rate $\epsilon = \nu \int_0^\infty k^2 E(k)\,\mathrm{d}k$ is largely determined by the k^{-2} spectrum, even though for this region the dominant dynamics are inviscid. Using (4.13) it follows that

$$\epsilon \sim \nu \int_0^{l_\nu^{-1}} k^2 E(k)\,\mathrm{d}k \sim \nu^{\frac{1}{2}} B^{\frac{4}{3}}. \tag{5.4}$$

Since $B \propto \beta u_0^2/L$, and $\beta = t\,\mathrm{d}U_1/\mathrm{d}x_2$, it follows that, in the RDT limit, ϵ is determined by the shear, and only reaches a steady value if the small-scale energy spectrum also reaches a steady state (i.e. B is constant).

At low or moderate Reynolds numbers without shear, where $E(k) = o(k^{-2})$, the dissipation rate is determined by the large scales (typically $\lambda/L \lesssim \frac{1}{3}$, where $\epsilon \sim \nu u_0^2/\lambda^2$), and consequently the ratio of λ/L or $\epsilon u_0^3/L$ is sensitive to Reynolds number and the form of the spectrum. However, in the presence of shear, even at moderate Reynolds number, this theory shows that the dissipation is determined by smaller scales, which have a general form that is less sensitive to the detailed form of the large-scale spectrum, and the ratio $\epsilon u_0^3/L$ varies slowly ($\propto (\nu/Lu_0)^{\frac{1}{3}}$) with Reynolds number.

This reasoning suggests why formulae and models for the rate of dissipation, which are ostensibly based on the concepts of very high-Reynolds-number turbulence, are approximately applicable in shear flows at moderate Reynolds number.

This paper owes much to lectures and conversions on turbulence by G. K. Batchelor, A. A. Townsend and many colleagues around the world. F. Hussain, P. A. Durbin and M. J. Lee kindly read the manuscript (but the errors are ours). J.C.R.H. acknowledges the hospitality and stimulation of visits to the Center of Turbulence Research at Stanford and NASA Ames, and of Ecole Centrale de Lyon. D.J.C. acknowledges financial support from NERC and SERC.

REFERENCES

ADRIAN, R. J. & MOIN, P. 1988 Stochastic estimation of organized turbulent structure: homogeneous shear flow. *J. Fluid Mech.* **190**, 531–559.

AUTON, T. R., HUNT, J. C. R. & PRUD'HOMME, M. 1988 The force exerted on a body in inviscid unsteady non-uniform rotational flow. *J. Fluid Mech.* **197**, 241–257.

BATCHELOR, G. K. 1953 *The Theory of Homogeneous Turbulence.* Cambridge University Press, 197 pp.

BATCHELOR, G. K. 1955 The effective pressure exerted by a gas in turbulent motion. In *Vistas in Astronomy* (ed. A. Beer), vol. 1, pp. 290–295. Pergamon.

BATCHELOR, G. K. 1967 *An Introduction to Fluid Dynamics.* Cambridge University Press, 615 pp.

BATCHELOR, G. K. & PROUDMAN, I. 1954 The effects of rapid distortion of a fluid in turbulent motion. *Q. J. Mech. Appl. Maths* **7**, 83–103.

BATCHELOR, G. K. & PROUDMAN, I. 1956 The large-scale structure of homogeneous turbulence. *Phil. Trans. R. Soc. Lond.* A **248**, 369–405.

BRADSHAW, P. 1967 The turbulence structure of equilibrium boundary layers. *J. Fluid Mech.* **29**, 625–645.

BRITTER, R. E., HUNT, J. C. R. & MUMFORD, J. C. 1979 The distortion of turbulence by a circular cylinder. *J. Fluid Mech.* **92**, 269–301.

BRITTER, R. E., HUNT, J. C. R. & RICHARDS, K. J. 1981 Analysis and wind-tunnel studies of speed-up, roughness effects and turbulence over a two-dimensional hill. *Q. J. R. Met. Soc.* **107**, 91–110.

CAMBON, C. & JACQUIN, L. 1989 Spectral approach to non-isotropic turbulence subjected to rotation. *J. Fluid Mech.* **202**, 295–318.

CARRUTHERS, D. J., FUNG, J. C. H. & HUNT, J. C. R. 1989 The emergence of characteristic eddy motion in turbulent shear flows. *Proc. Organized Structures and Turbulence in Fluid Mechanics* (ed. M. Lesieur & O. Métais).

CARRUTHERS, D. J. & HUNT, J. C. R. 1986 Velocity fluctuations near an interface between a turbulent region and a stably stratified layer. *J. Fluid Mech.* **165**, 475–501.

CHAMPAGNE, F. H., HARRIS, V. G. & CORRSIN, S. 1970 Experiments on nearly homogeneous turbulent shear flow. *J. Fluid Mech.* **41**, 81–139.

COMTE-BELLOT, G. & MATHIEU, J. 1987 (eds.) *Advances in Turbulence. Proc. First European Turbulence Conference, Lyon, July 1986.* Springer.

CRAYA, A. 1958 Contribution à l'analyse de la turbulence associée à des vitesses moyennes. *P.S.T. Ministère de l'Air*, vol. 345.

CROW, S. C. 1968 Turbulent Rayleigh shear flow. *J. Fluid Mech.* **32**, 113–120.

DAVIDSON, P. A., HUNT, J. C. R. & MOROS, A. 1968 Turbulent recirculating flows in liquid metal magnetohydrodynamics. *Prog. Astronaut. Aeronaut.* **111**, 400–420.

DEISSLER, R. G. 1968 Effects of combined two-dimensional shear and normal strain on weak locally homogeneous turbulence and heat transfer. *J. Math. Phys.* **47**, 320–331.

DRITSCHEL, D. 1989 Contour dynamics and contour surgery: numerical algorithms for extended, high-resolution modelling of vortex dynamics in two-dimensional, inviscid, incompressible flows. *Comput. Phys. Rep.* **10**, 77–146.

DURBIN, P. A. 1981 Distorted turbulence in axisymmetric flow. *Q. J. Mech. Appl. Maths* **34**, 489–500.

DURBIN, P. A. & HUNT, J. C. R. 1980 On surface pressure fluctuations beneath turbulent flow round bluff bodies. *J. Fluid Mech.* **100**, 161–184.

DUSSAGE, J. P. & GAVIGLIO, J. 1981 Bulk dilatation effects on Reynolds stresses in the rapid expansion of a turbulent boundary layer at supersonic speeds. *Proc. Symp. Turbulent Shear Flows, Davis*, pp. 2.33–2.38.

FERRÉ, J. A. & GIRALT, F. 1989 Pattern-recognition analysis of the velocity field in plane turbulent wakes. *J. Fluid Mech.* **198**, 27–64.

GARTSHORE, I. S., DURBIN, P. A. & HUNT, J. C. R. 1983 The production of turbulent stress in a shear flow by irrotational fluctuations. *J. Fluid Mech.* **137**, 307–329.

GASTER, M., KIT, E. & WYGNANSKI, I. 1985 Large-scale structures in a forced turbulent mixing layer. *J. Fluid Mech.* **150**, 23–39.

GILBERT, A. 1988 Spiral structures and spectra in two-dimensional turbulence. *J. Fluid Mech.* **193**, 475–497.

GOLDSTEIN, M. E. 1978 Unsteady vortical and entropic distortion of potential flow round arbitrary obstacles. *J. Fluid Mech.* **89**, 433–468.

GOLDSTEIN, M. E. & ATASSI, H. 1976 A complete second-order theory for the unsteady flow about an airfoil due to a periodic gust. *J. Fluid Mech.* **74**, 741–765 (and Corrigendum, **91**, 1979, 788).

GOLDSTEIN, M. E. & DURBIN, P. A. 1980 The effect of finite turbulence spatial scale on the amplification of turbulence by a contracting stream. *J. Fluid Mech.* **98**, 473–508.

GRAHAM, J. M. R. 1976 Turbulent flow past a porous plate. *J. Fluid Mech.* **73**, 565–591.

HAYAKAWA, M. & HUSSAIN, F. 1989 Three-dimensionality of organized structures in a plane turbulent wake. *J. Fluid Mech.* **206**, 375–404.

HO, C. M. & HUERRE, P. 1984 Perturbed free shear layers. *Ann. Rev. Fluid Mech.* **16**, 365–424.

HUNT, J. C. R. 1973 A theory of turbulent flow round two-dimensional bluff bodes. *J. Fluid Mech.* **61**, 625–706.

HUNT, J. C. R. 1978 A review of the theory of rapidly distorted turbulent flow and its applications. *Proc. XIII Biennial Fluid Dynamics Symp., Kortowo, Poland, Fluid Dyn. Trans.* **9**, 121–152.

HUNT, J. C. R. 1984 Turbulence structure in thermal convection and shear-free boundary layers. *J. Fluid Mech.* **138**, 161–184.

HUNT, J. C. R. 1987 Vorticity and vortex dynamics in complex turbulence flow. Proc. CANCAM (Canadian Congress of Applied Mechanics, London, Ontario). *Trans. Can. Soc. Mech. Engng* **11**, 21–35.

HUNT, J. C. R. 1988 Studying turbulence using direct numerical simulation: 1987 Center for Turbulence Research NASA Ames/Stanford Summer Programme. *J. Fluid Mech.* **190**, 375–392.

HUNT, J. C. R. & GRAHAM, J. M. R. 1978 Free-stream turbulence near plane boundaries. *J. Fluid Mech.* **84**, 209–235.

HUNT, J. C. R., NEWLEY, T. M. J. & WENG, W.-S. 1989 Analysis and computation of turbulent boundary layers with varying pressure gradients. *Joint IMA-SMAI Conf. on Computational Methods in Aeronautical Fluid Dynamics, University of Reading, April 1987* (ed. P. Stow). Oxford University Press.

HUSSAIN, A. K. M. F. 1983 Coherent structures – reality and myth. *Phys. Fluids* **26**, 2816–2850.

HUSSAIN, A. K. M. F. 1986 Coherent structures and turbulence. *J. Fluid Mech.* **173**, 303–356.

JEANDEL, D., BRISON, J. F. & MATHIEU, J. 1978 Modelling methods in physical and spectral space. *Phys. Fluids* **21**, 169–182.

KAWAI, H. 1990 Pressure fluctuations on an upwind surface of two-dimensional square prisms in a turbulent flow. *J. Fluid Mech.* (submitted).

KIDA, S. & HUNT, J. C. R. 1989 Interaction between turbulence of different scales over short times. *J. Fluid Mech.* **201**, 411–445.

KOMORI, S., UEDA, H., OGINO, F. & MIZUSHINA, T. 1983 Turbulence structure in stably stratified open channel flow. *J. Fluid Mech.* **130**, 13–26.

LANDAHL, M. T. 1984 Coherent structures in turbulence and Prandtl's mixing length theory. *Z. Flugwiss. Weltraumforsch.* **8**, 233.

LANDAHL, M. T. 1990 Theoretical model for VITA-educed coherent structures in the wall region of a turbulent boundary layer. *Proc. 2nd Stanford Summer School*, pp. 209–220.

LAUNDER, B. E., REECE, G. J. & RODI, W. 1975 Progress in the development of a Reynolds stress turbulence closure. *J. Fluid Mech.* **68**, 537–566.

LAUNDER, B. E. & SPALDING, D. B. 1972 *Mathematical Models of Turbulence.* Academic.

LEE, M. J. 1985 Ph.D. thesis. Mech. Eng. Stanford University.

LEE, M. J. & HUNT, J. C. R. 1989 The structure of sheared turbulence near a boundary. *Center for Turbulence Research, Stanford, Rep.* CTR-S88, pp. 221–242.

LEE, M. J., KIM, J. & MOIN, P. 1987 Turbulent structure at high shear rate. *Turbulent Shear Flows, 6,* pp. 22.6.1–22.6.6. Springer.

LEITH, C. E. 1978 Objective methods for weather prediction. *Ann. Rev. Fluid Mech.* **10**, 107–128.

LESIEUR, M. 1987 *Turbulence in Fluids.* Martinus Nijhoff.

LESIEUR, M. & MÉTAIS, O. 1989 *Proc. Pole European Pilote de Turbulence (PEPIT), ERCOFTAC Summer School, Lyon, July 1989.*

LESLIE, D. C. 1973 *Developments in the Theory of Turbulence.* Clarendon.

LESSEN, M. 1979 On the power laws for turbulent jets, wakes and shearing layers and their relationship to the principle of marginal instability. *J. Fluid Mech.* **88**, 535–540.

LIU, J. T. C. 1989 Contributions to the understanding of large-scale coherent structures in developing free turbulent shear flows. *Adv. Appl. Mech.* **26**, 183–309.

LUMLEY, J. 1965 The structure of inhomogeneous turbulent flows. *Proc. Intl Coll. on Radio Wave Propagation* (ed. A. M. Yaglom & V. I. Takasky), *Dokl. Akad. Nauk. SSSR,* 166–178.

LUMLEY, J. L. 1978 Computational modelling of turbulent flows. *Adv. Appl. Mech.* **18**, 126–176.

MASON, P. J. & KING, J. C. 1985 Measurements and predictions of flow and turbulence over an isolated hill of moderate slope. *Q. J. R. Met. Soc.* **111**, 617–640.

MAXEY, M. R. 1978 Aspects of unsteady turbulent shear flow. Ph.D. dissertation, University of Cambridge.

MAXEY, M. R. 1982 Distortion of turbulence in flows with parallel streamlines. *J. Fluid Mech.* **124**, 261–282.

MOFFATT, H. K. 1967 On the suppression of turbulence by a uniform magnetic field. *J. Fluid Mech.* **28**, 571–592.

MOFFATT, H. K. 1984 Simple topological aspects of turbulent vorticity dynamics. In *Turbulence and Chaotic Phenomena in Fluids* (ed. T. Tatsumi), pp. 223–230. Elsevier.

MONIN, A. S. & YAGLOM, A. M. 1971 *Statistical Theory of Turbulence,* vol. II. MIT Press.

MUMFORD, J. C. 1982 The structure of the large eddies in fully developed turbulent shear flows. Part 1. The plane jet. *J. Fluid Mech.* **118**, 241–268.

MURAKAMI, S. & MOCHIDA, A. 1988 3D numerical simulation of airflow around a cubic model by means of a k–ϵ model. *J. Wind. Engng Indust. Aerodyn.* **31**, No. 2.

PEARSON, J. R. A. 1959 The effect of uniform distortion on weak homogeneous turbulence. *J. Fluid Mech.* **5**, 274–288.

PHILLIPS, O. M. 1955 The irrotational motion outside a free turbulent boundary. *Proc. Camb. Phil. Soc.* **51**, 220–229.

RODI, W. 1988 Recent developments in turbulence modelling. *Proc. 3rd Intl Symp. on Refined Flow Modelling and Turbulence Measurements, Tokyo, July.*

ROGALLO, R. S. 1981 Numerical experiments in homogeneous turbulence. *NASA Tech. Memo.* 81315.

ROGERS, M. M. 1990 The response of a passive scalar field to a mean scalar gradient in rapidly sheared turbulent flow. *Phys. Fluids* (submitted).

ROGERS, M. M. & MOIN, P. 1987 The structure of the vorticity field in homogeneous turbulent flows. *J. Fluid Mech.* **176**, 33–66.

RUDERICH, R. & FERNHOLZ, H. H. 1986 An experimental investigation of a turbulent shear flow with separation, reverse flow, and reattachment. *J. Fluid Mech.* **163**, 283–322.

SAFFMAN, P. G. 1967 Note on decay of homogeneous turbulence. *Phys. Fluids* **10**, 1349.

SAVILL, A. M. 1987 Recent developments in rapid-distortion theory. *Ann. Rev. Fluid Mech.* **19**, 531–570.

SREENIVASAN, K. R. 1985 The effect of a contraction on a homogeneous turbulent shear flow. *J. Fluid Mech.* **154**, 187–213.

SREENIVASAN, K. R. & NARASIMHA, R. 1978 Rapid distortion of axisymmetric turbulence. *J. Fluid Mech.* **84**, 497–516.

TAYLOR, G. I. & BATCHELOR, G. K. 1949 The effect of wire gauze on small disturbances in a uniform stream. *Q. J. Mech. Appl. Maths* **2**, 1–29.

TENNEKES, H. 1988 Numerical weather prediction: illusions of security, tales of imperfection. *Weather* **43**, 165–169.

TENNEKES, H. & LUMLEY, J. L. 1971 *A First Course in Turbulence*. MIT Press.

THOMAS, N. H. & HANCOCK, P. E. 1977 Grid turbulence near a moving wall. *J. Fluid Mech.* **82**, 481–496.

TOWNSEND, A. A. 1961 Equilibrium layer and wall turbulence. *J. Fluid Mech.* **11**, 87–120.

TOWNSEND, A. A. 1970 Entrainment and the structure of turbulent flow. *J. Fluid Mech.* **41**, 13–46.

TOWNSEND, A. A. 1976 *Structure of Turbulent Shear Flow*. Cambridge University Press.

TOWNSEND, A. A. 1980 The response of sheared turbulence to additional distortion. *J. Fluid Mech.* **98**, 171–191.

TUCKER, H. J. & REYNOLDS, A. J. 1968 The distortion of turbulence by irrotational plane strain. *J. Fluid Mech.* **32**, 657–673.

UZKAN, T. & REYNOLDS, W. C. 1967 A shear-free turbulent boundary layer. *J. Fluid Mech.* **28**, 803–821.

WEBER, W. 1868 Über eine Transformation der hydrodynamischen Gleichungen. *J. Reine Angew. Math.* **68**, 286.

WRAY, A. & HUNT, J. C. R. 1989 Algorithms for classification of turbulent structures. In *Proc. IUTAM Symp. on Topological Fluid Mechanics*. Cambridge University Press.

WYNGAARD, J. C. & COTE, O. R. 1972 Modelling buoyancy driven mixed layers. *J. Atmos. Sci.* **33**, 1974–1988.

ZEMAN, O. & JENSEN, N. O. 1987 Modification of turbulence characteristics in flow over hills. *Q. J. R. Met. Soc.* **113**, 55–80.